Hindawi
Aquaculture Nutrition
Volume 2022, Article ID 1154558, 22 pages
https://doi.org/10.1155/2022/1154558

Research Article

The Immunostimulant Effects of *Isochrysis galbana* Supplemented Diet on the Spleen of Red Hybrid Tilapia (*Oreochromis* spp.) Evaluated by Nuclear Magnetic Resonance Metabolomics

Muhammad Safwan Ahamad Bustamam,[1] **Hamza Ahmed Pantami**,[2] **Amalina Ahmad Azam**,[3] **Khozirah Shaari**,[1] **Chong Chou Min**,[4] **and Intan Safinar Ismail**[1,5]

[1]*Natural Medicine and Products Research Laboratory, Institute of Bioscience, Universiti Putra Malaysia, 43400 UPM Serdang, Selangor, Malaysia*
[2]*Chemistry Department, Gombe State University, P.M .B 127 Gombe, Gombe State, Nigeria*
[3]*Center for Healthy Ageing and Wellness (H-Care), Faculty of Health Sciences, Universiti Kebangsaan Malaysia Campus Kuala Lumpur, Jalan Raja Muda Abdul Aziz, 50300 Kuala Lumpur, Malaysia*
[4]*Department of Aquaculture, Faculty of Agriculture, Universiti Putra Malaysia, 43400 Serdang, Selangor, Malaysia*
[5]*Department of Chemistry, Faculty of Science, Universiti Putra Malaysia, 43400 Serdang, Selangor, Malaysia*

Correspondence should be addressed to Intan Safinar Ismail; safinar@upm.edu.my

Received 10 October 2021; Accepted 7 March 2022; Published 11 April 2022

Academic Editor: Ayşegül Kubilay

Significant measures at improving aquaculture health have to be taken since disease outbreaks commonly occur in the fast-growing aquaculture industry. This study aimed to determine the immunomodulatory properties of an indigenous Malaysian microalgae species, *Isochrysis galbana* (IG), on red hybrid tilapia (*Oreochromis* spp.). Then, the potential biomarkers for immunomodulatory properties were identified through metabolic changes in the spleen using the proton nuclear magnetic resonance (^{1}H NMR) metabolomics approach. IG was cultivated in an indoor annular photobioreactor before being harvested and freeze-dried into dried biomass. The dried IG biomass was incorporated into four experimental diets in concentrations of 0% (diet A), 0.6% (diet B), 1.3% (diet C), 2.5% (diet D), and 5.0% (diet E) basal feed per kg. After 14 days of feeding, diet D has consistently improved the immune responses of innate immunity such as phagocytosis ($P > 0.05$), respiratory burst ($P < 0.05$), and lymphoproliferation ($P < 0.05$) activities which might have helped in maintaining the overall health status of red hybrid tilapia. The orthogonal partial least squares (OPLS) model between diets D and A indicated three important metabolites, namely, isoleucine, glutamate, and tyrosine, have significantly been upregulated when compared to the control. Meanwhile, IG supplementation also resulted in lower concentrations of various metabolites in the spleen including α/β-glucose, choline, hypoxanthine, adenosine, and inosine. Hence, the application of metabolomics tools has proved the potential of IG-incorporated fish diet by strongly influencing the metabolic condition in red hybrid tilapia spleen cells and further boosting the immune response and health status in improving aquaculture health.

1. Introduction

Nowadays, aquaculture production provides about 50% of the global fish supply while the other half is provided by fisheries [1]. In Malaysia, tilapia (*Oreochromis* spp.) is the second highest harvested freshwater fish, with a total annual production of 33,404 tonnes. The estimated wholesale value of this species was RM 346 million [2], which indicates the importance of tilapia farming in Malaysia, However, world aquaculture production is vulnerable, and an increase of disease outbreaks has been reported due to culture intensification, resulting in partial or total loss of production [3]. Hence, the fore of research is using immunostimulants as a suitable alternative to strengthen both the specific and nonspecific fish immune systems in aquaculture [4, 5]. However, the recommended dose of each immunostimulant differs based on the plant, fish species, and route of administration [6].

Microalgae are categorized as eukaryotic organisms with unicellular photosynthetic ability and exist in a different range of morphologies and characteristics. Supplementation of several microalgae such as *Chlorella vulgaris* and *Spirulina platensis* in fish diet has been proven in stimulating the fish immune system [7–9]. *Isochrysis galbana* (IG) is a marine microalgae species classed under Isochrysidales order in the same group of Haptophyta division (Phylum). The advantage of IG is due to its less cell wall, rapid growth, and high endurance to high temperature and outdoor environment [10–12], which makes it possible to be cultivated under unpredictable tropical conditions [13]. IG is one of the high-quality microalgae used in the food industry due to its high lipid content (20-30%) mainly from PUFA, namely, eicosapentaenoic acid (EPA) and docosahexaenoic acid (DHA) [14]. It also contains a high total carotenoid mainly contributed by fucoxanthin [15, 16]. These traits of IG make it one of the most highly demanded microalgae for aquaculture.

Various immune functions at the metabolic stage are bioenergy costly, demanding accurate control of cellular metabolic pathways to protect against contaminants, and sustain tissue homeostasis for the organism's lifespan. Since immune cells lack significant nutritional sources, these effector responses can only be preserved if immune cells can significantly improve their microenvironment absorption of glucose, amino acids, and fatty acids [17]. Previous studies have reported several microalgae with immune responses and disease resistance properties, but none of them reported the potential of IG as natural immunostimulants. In addition, research on the immunomodulatory impact of microalgae on fish at the metabolic stage has yet been published. Metabolomics provides a systematic understanding of metabolic changes and interference of biological mechanisms related to environmental influences on fish health and welfare and fish feeding [18, 19]. NMR is the most frequently applied in metabolomics because of its high reproducibility, non-destructive, broad range of detection in a single type of analysis, and gives detailed structural knowledge for identification [20]. The current research is the first work in which a metabolomic strategy has been utilized to evaluate the metabolite level of the spleen cell suspension in red hybrid tilapia fed with IG-incorporated diet.

2. Materials and Methods

2.1. Microalgae Growth Production. Isochrysis galbana (UPMC-A0009) used in this study was procured from Microalgal Production Laboratory, Aquatic Animal Health Unit, Faculty of Veterinary Medicine, Universiti Putra Malaysia in April 2017. The pure culture was sustained at 23°C in an environmental chamber (Sanyo, Osaka, Japan). The growth of IG was initiated on a 3 mL aliquot of the pure culture with 20 mL Conway medium prepared in filtered (5 μm) and sterilized seawater [21]. It was eventually scaled up to 90 L with constant aeration in a 120 L annular photobioreactor, receiving artificial light–dark cycles (12–12) at intensity 150 mol/m2/s. The growth of the microalgae was monitored using the biomass weight and cell count. The biomass weight was obtained by dividing the dry weight of the filtered biomass by the filtrate volume [22]. Daily cell counts were done using a Neubauer hemocytometer (Assistant, Germany) on a well-mixed sample. The microalgae were harvested during their late exponential growth period of 15 days by centrifuging them at 8000 rpm, as described by Aguilera-Sáez et al. [23], with some adjustments. Then, the biomass collected was freeze-dried (Scanvac, Denmark) and deposited until used at -80°C.

2.2. Diets Preparation. Star Feed TP-1 (Star Feedmills (M), Sdn Bhd, Selangor, Malaysia) commercial diet was used as a basal feed with an estimated 32% crude protein content, 3% crude fat, 14.6% ash, 12% moisture, and 3% fibre. Powder of harvested IG was combined with a commercial basal diet and some distilled water to obtain four homogenized concentrations: 0.6% (diet B), 1.3% (diet C), 2.5% (diet D), and 5.0% (diet E), of dry biomass microalgae per kg basal feed, and control (diet A) without microalgae. The formulated diets were then manually pressed inside a 5 mL modified syringe into pellet form and cut separately into 0.5 cm size. The formulated pellets were dried in the oven at 35°C for 24 hours before being deposited at room temperature in sterile cap bottles.

2.3. Experimental Design. Sixty juvenile red hybrid tilapia fish, with an average weight of 55.6 ± 0.12 g (mean ± SD), were acquired from Taman Pertanian Universiti (TPU) fish hatchery, UPM and transported to the fish hatchery of the Laboratory of Marine Biotechnology (MARSLAB), Institute of Bioscience (IBS), UPM. The fish were acclimatized for ten days in a 500 liter (L) fiberglass aerated tank filled with de-chlorinated freshwater. During acclimatization, fish were fed with a basal diet throughout the experiment at 1% of body weight in two equal parts twice a day at 9.00 a.m. and 5.00 p.m. Water was changed every three days at the rate of 30%, and water quality was monitored daily throughout the experiment. The temperature was maintained at 28 ± 1°C, dissolved oxygen concentration more than 4.0 mg/L, and pH 8.0 ± 1 by YSI Professional Plus (Yellow Spring Instrument, USA). Following acclimatization, the fish were divided into five different experimental diets (A, B, C, D, and E) groups as described. During the feeding trial, the water temperature was 26.1 ± 0.1°C, dissolved oxygen was

4.94 ± 0.23 mg/L, and the pH range was 7.52 ± 0.22. All experiments were carried out in conjunction with the Institutional Animal Care and Use Committee of Universiti Putra Malaysia (UPM) (IACUC/AUP- R080/2018).

After the acclimatization period, fish were randomly divided into five experimental groups and fed with four different experimental diets (B, C, D, and E) and a control (A). Each group was divided into six identical 40 L rectangular glass aquariums (0.6 m diameter and 0.75 m height) at a density of 2 fish per aquarium (6 aquariums per diet). During the feeding period of 14 days, fish in each group were gently hand-fed with the diet at 1% of body weight at 9:00 a.m. and 5:00 p.m. per day. The feeding was carefully done and observed to make sure the feeds were all consumed. Water quality parameters were monitored throughout the experiment. During the feeding period, the water temperature, dissolved oxygen, and pH ranged were 26.1 ± 0.1°C, 4.94 ± 0.23 mg/L, and 7.52 ± 0.22, respectively.

2.4. Sample Collection for Immunological Measurement. The experimental fish was placed in a tank with MS-222 at a lethal level (500 mg/L) for at least 3 min [24]. The dead fish was then passed to the dissection station, where freshly cleaned tools were used to excise the spleen from the body. The spleen was then divided into two parts whereby the first part of the tissue was placed in an individual, prelabelled vial, and flash-frozen in liquid nitrogen for NMR analysis. The second part of the tissue was weighed and meshed by gently pressing it through sterile cell strainers of 40 μm nylon mesh together with 5 mL cold 1× phosphate buffered saline (PBS). The supernatant was collected and centrifuged at 1800 rpm for 10 minutes to remove PBS. The cell pellet obtained was mixed with freezing media and aliquoted before storage at -80°C until used.

2.5. Phagocytosis Activity. Phagocytosis activity of spleen cell suspension was determined based on Ai et al. [25] with some modifications. A suspension of 100 μL spleen leucocytes (1×10^5 cells/mL) was placed in a sterile microcentrifuge before being mixed with 100 μL yeast suspension (Baker's yeast, Type II, Sigma-Aldrich, USA) at concentration 1×10^7 cells/mL and allowed to incubate for 30 min at 25°C. Following incubation, 5 μl of the suspension was dropped on a clean microscope slide precoated with 10% Poly L-Lysine (Sigma-Aldrich, USA) before uniformly spreading to produce a smear. After air-drying, the slides were fixed in methanol for 1 minute, then in May-Grunwald solution (5 minutes) and stained with 7% Giemsa (20 minutes) before being rinsed and redried. The percentage of phagocytes was determined by observing 100 phagocytes from a random region on the slide under a microscope (Nikon Eclipse 80i, Japan).

2.6. Respiratory Burst Activity. The respiratory burst activity (RBA) of the phagocytes was evaluated by nitroblue tetrazolium (NBT, Sigma, USA) assay based on the method of Secombes [26] with modifications. A hundred microliters of spleen cell suspension (1×10^5 cells/mL) in 1x PBS were deposited in 96 microplates, then mixed with 100 μl of 5 mg/ml zymosan A (Sigma-Aldrich, USA) along with a control (spleen cell without zymosan) before it stands for 30 min at room temperature. The suspension was centrifuged at 1800 rpm in a microplate centrifuge (Thermo Fisher Scientific Inc., Waltham, MA USA). The microplates were washed three times with discard zymosan before being stained with 100 μL of a nitroblue tetrazolium (NBT) solution (2 mg/mL) and stood for 30 min at room temperature. The suspension was then centrifuged to discard the supernatant before the reaction was stopped by adding 100 μL of methanol. Methanol was discarded through microplate centrifugation followed by the addition of 120 μL of 2 M potassium hydroxide (KOH) and 140 μL dimethyl sulfoxide (DMSO). The colour was subsequently measured at 630 nm with a spectrophotometer (Thermo, USA) using KOH and DMSO as a blank. The result of RBA for each sample was expressed as a stimulated activity with zymosan deducted from the basal activity without zymosan.

2.7. Lymphoproliferation Assay. A hundred microliters of spleen leucocytes (1×10^5 cells/mL) was deposited in a sterile 96-well microplate. Then, 100 μL of the mitogen phytohemagglutinin (PHA; Sigma-Aldrich, USA) was prepared in complete media (10% Fetal Bovine Serum: 90% Dulbecco's Modified Eagle's medium) at the concentration of 10 μg/mL before being added into the cells to activate T-cells. Both treated and untreated cells (without PHA) were incubated for 48 hours at 25°C in a 5% CO_2 incubator. After incubation, the cells were counted manually using a haemacytometer under the microscope (Zeiss Axioscope, Germany). The same procedure was repeated for mitogen lipopolysaccharide (LPS; Sigma-Aldrich, USA) at a concentration of 40 μg/ml to activate the B-cells.

2.8. ^{1}H NMR Spectroscopic Analysis. The pre-weighed spleen was thawed and mixed with 200 μl of 99.9% deuterium oxide (D_2O) containing 90 mM KH_2PO_4 buffer solution (pH 6.0) and 0.1% trimethylsilylpropionic acid-d4 sodium salt (TSP) as the internal reference standard. The tissue was homogenized using a glass rod before being centrifuged at 10,000 rpm for 10 min at room temperature. The resultant clear supernatant was slowly pipetted out into a 3 mm standard NMR tube (Norell, USA) and sent for analysis on a Bruker 700 MHz spectrometer equipped with a TCI CryoProbe (Bruker Biospin, Billerica, MA, USA). The spectra were obtained using the Carr–Purcell–Meiboom–Gill (CPMG) pulse sequence to suppress the signals of proteins [27] using a 90° pulse (6.6 μs at a transmitter power of 58 dB), a spectral width of 10 504 Hz, an acquisition time of 3.1 s using 48 k data points, 128 scans, and a relaxation delay of 4.0 s. Deuterium oxide was used as the internal lock solvent, and the residual solvent peak was suppressed using a 64 scan PRESAT sequence, with a total acquisition time of 3.53 min.

The 2D NMR spectra such as J-resolved (JRES) and HSQC were acquired using a similar instrument at room temperature (25°C) using 24 scans, 1 k data points at 256 increments, a spectral width of 16 ppm in dimensions, and a relaxation delay of 2 s.

2.9. Pre-Processing of NMR Spectra. The pre-processing of all ^{1}H NMR spectra was done manually involving phasing baseline correction before referenced to the internal standard (TSP) at 0.00 ppm using Chenomx NMR Suite 5.1 Professional (Edmonton, Canada). The spectral regions from 0.3 to 10 ppm were normalized to the total sum of the spectral intensity after excluding residual water (4.7-4.9 ppm) and binned into an integrated bucket of 0.04 ppm in width. The generated binned data in a table sheet was then visualized in a multivariate analysis using SIMCA-P 14.1 (Umetrics, Umea^o, Sweden).

The dataset was set to a Pareto scale before executing the Principal Component Analysis (PCA) and OPLS models by SIMCA. In the score plot generated, each variable was represented as an individual spleen sample, which allowed the observation of the classification behaviour of spleen samples along with the two main principal components of PC1 and PC2. The metabolites responsible for the groups' separation could be identified based on the variables that appeared in the loading plots, represented as individual bins of the ^{1}H NMR data. The validation and fitting of the generated models were evaluated based on three-fold approach, including 100 permutation tests, computation of R2Y, Q2Y, and CV-ANOVA values [28].

2.10. Statistical Analysis. The normality of the bioactivity data was evaluated based on the Shapiro-Wilk test before statistical analysis with *P*-value measured greater than 0.05 indicated as the data was normally distributed. Statistical analysis was performed using SPSS 16.0 (SPSS Inc., Michigan Avenue, Chicago, IL, USA). Significant differences between the samples were determined using one-way analysis of variance (ANOVA) followed by Duncan's post hoc test at a confidence interval of 95%. A *P*-value less than 0.05 was considered significant.

3. Results and Discussion

3.1. Phagocytosis Activity. Innate immunity is of utmost importance in teleosts since their adaptive immune response is less evolved than in mammals. Phagocytosis is a common innate immune response mechanism by phagocyte cells involving monocytes, macrophages, neutrophils, mast cells, dendritic cells, and nonspecific cytotoxic cells [29–31]. Phagocyte cells are responsible for defending the host by ingesting toxic foreign particles, including dead or dying cells [30, 32, 33]. Phagocytosis begins as phagocyte cells engulf recognized particles, including pathogens, aged red blood cells, and foreign substances, by attaching them to their surface and internalizing them into phagosomes formed around the objects engulfed [34]. In the present study, phagocytic activity is defined as the percentage of leukocytes that engulfed yeast cells within a total of 100 leukocytes counted in the smear.

The impact of IG-supplemented diets on the phagocytosis activity is not dose-dependent and not significant except for group B, as displayed in Figure 1. The highest percentage of phagocytosis was observed in group B of 0.63% IG, followed by D (2.5% IG) with 55% and 41% accretion, compared with the control (group A) after 14 days of feeding treatment. Other groups showed no significant difference with less than 10% increment of activity compared to the control. It was mentioned that successful administration of any immunostimulant demands the use of an accurate dietary inclusion level over a sufficient period of time [35]. There was yet no study reported on the effect of dietary IG on the phagocytosis activity in tilapia. However, the potential of other microalgae in phagocytosis activity has been revealed. For instance, Galal et al. [8] found that 10% *Chlorella vulgaris* incorporated diet significantly ($P < 0.05$) increased phagocytic activity in tilapia after 15 and 30 days of the feeding period. Oral administration of 10 mg *Spirulina platensis* suspension to tilapia also enhanced the phagocytic activity more than vaccine-treated [36]. In another study, significant dose-dependent stimulation of phagocytic activity was observed on head kidney leucocytes of gilthead seabream fed with *Phaeodactylum*-incorporated diet. However, not much difference was observed with *Tetraselmis*- and *Nannochloropsis*-incorporated diets than the control [37].

The manual count of phagocytic cells using an electron microscope as applied in the present study has several disadvantages. During the counting process, the glass slide's scanning movement introduced overlapping scanning regions resulting in counting errors, in which the cells might not be uniformly distributed across the smear. These issues can be overcome by using the flow cytometry method, which is more accurate and less time consuming [38]. Unfortunately, the flow cytometer was not available to be used for the current study.

3.2. Respiratory Burst Activity (RBA). The ability of leukocytes to destroy invading pathogenic agents is one of the important defence mechanisms. A mechanism known as leukocyte respiratory burst activity involves professional phagocytes such as neutrophils, macrophages, dendritic cells, and monocytes, which also work as reactive oxygen species (ROS) producers [39]. ROS is predominantly formed in the mitochondria, peroxisomes, plasma membrane, and cytoplasm. Oxygen is less reactive due to biradical orbitals. However, the electron transfer or energy absorption can trigger the activation of ROS from molecular oxygen. ROS is comprised of oxygen-free radicals such as hydroxyl radical (HO•), superoxide anion (O_2•-), peroxyl (ROO•), alkoxyl (RO•), and nitric oxide (NO), as well as nonradical molecules such as oxygen, hydrogen peroxide (H_2O_2), and hydrochloric acid (HCl), and transition metals such as copper and iron [40, 41]. The leukocyte respiratory burst activity was used to indicate innate immunity since it was first discovered in mammals in the early 1930s. Some researchers noticed that high oxygen consumption happened during phagocytosis. Leukocytes increase their intracellular oxygen utilization during the phagocytosis of pathogens and subsequently produce diverse ROS. All ROS generated during phagocytosis with their by-products are very reactive and utilized as an immune system strategy to destroy invading pathogens. Respiratory or oxidative burst is a resting metabolic pathway in cells which is quickly activated to recognize the microbial agent. It is responsible for generating potent oxidizing

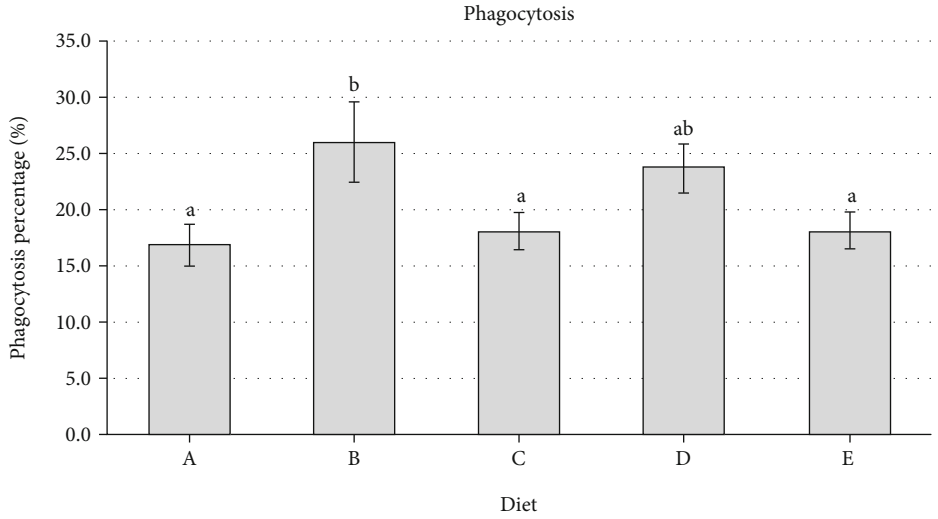

Figure 1: Effects of different IG diet concentrations on the phagocytosis activity in red hybrid tilapia (data are expressed as mean ± S.E.; means in the same column sharing a different superscript letter are significantly different ($P < 0.05$) determined by Duncan's test with $n = 6$).

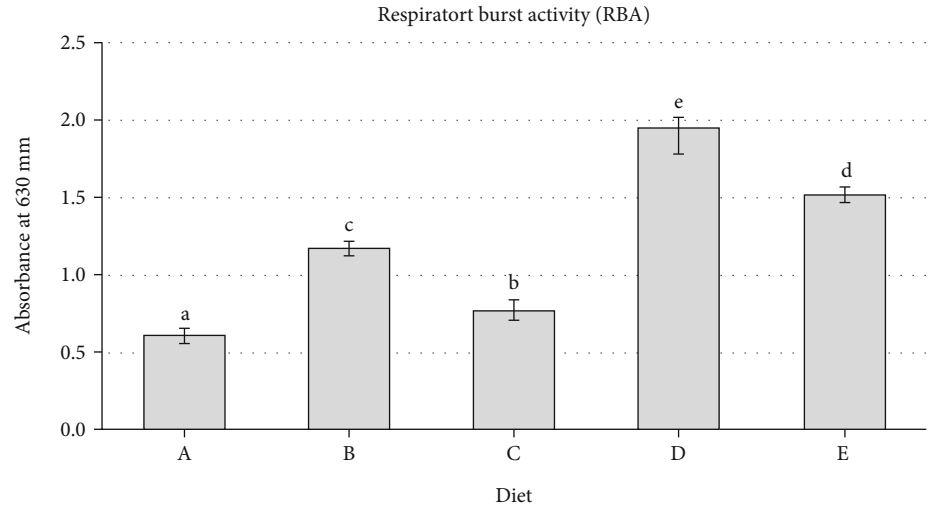

Figure 2: Effects of different IG diet concentrations on the respiratory burst activity in red hybrid tilapia. Data are expressed as mean ± S.E. (means in the same column sharing a different superscript letter are significantly different determined by Duncan's test ($P < 0.05$) with $n = 6$).

molecules or burst activity that functions to destroy microorganisms [39, 42, 43].

In the present study, zymosan particles made up of yeast cell walls were detected as a foreign pathogen and rapidly engulfed by phagocytic cells in the spleen leucocytes suspension. Nitroblue tetrazolium (NBT) chemical was used to determine the superoxide anion generated in various phagocytic cells. Current results in Figure 2 have exhibited a significant enhanced respiratory burst activity in the diet groups except for diet C when compared to the control. Diet D (2.5% IG) was marked as the highest respiratory burst activity with a value two times higher than the control.

Other studies also showed significant results of respiratory burst activity such as in juvenile great sturgeon fed with 10% *S. platensis* incorporated for eight weeks [44]. In another study, 0.13% of *Spirulina* in a basal diet demonstrated a positive immunity promoter for Nile tilapia in Egypt with significant enhanced respiratory burst activity after 12 weeks of feeding [45]. Similarly, Watanuki et al. [46] discovered the effects of 1 mg *Spirulina* in 0.1 ml suspension on carp expressing the highest superoxide anion production after three days of posttreatment.

However, the current results were not dose-dependent since diet D of 2.5% IG enhanced more superoxide production than diet E containing 5.0% IG. A similar pattern was also observed in Asian sea bass after being fed with different garlic (*Allium sativum*) supplemented diets for two weeks [47]. Treatment dose garlic at 10 g/kg feed gave the highest reading of superoxide anion production compared to 15 and 20 g/kg feed. In a different study, chitosan was a stimulating agent for phagocytosis and respiratory burst activity in cobia fish. Unfortunately, a high chitosan level of 6.0 g/kg caused inhibition of the activities, suggesting that the cells had become exhausted for some duration after being stimulated with a high concentration of chitosan [48]. It was supported by other studies which concluded that high chitosan

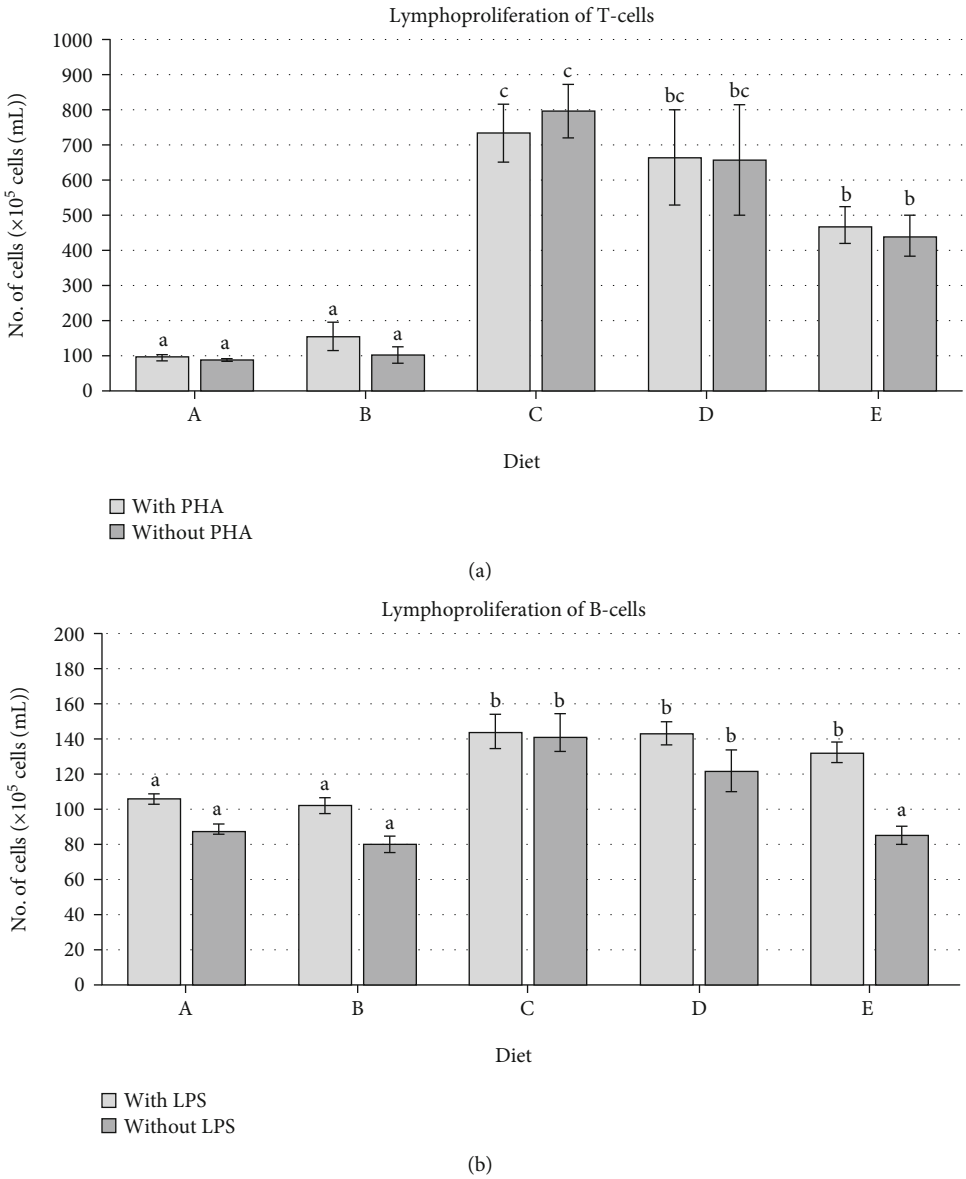

Figure 3: Effects of different IG diet concentrations on the (a) lymphoproliferation of T-cells and (b) B-cells in the spleen of red hybrid tilapia (data are expressed as mean ± S.E.; means in the same column sharing a different superscript letter are significantly different ($P < 0.05$) determined by Duncan's test with $n = 6$).

levels significantly inhibited phagocytosis and respiratory burst activity [49, 50]. However, the current study shows better results than long-term administration of dietary content of seaweed powders after demonstrating no significant differences regarding respiratory burst activity between control and different feeding period [35].

3.3. Lymphoproliferation Activity. Another essential approach for assessing the fish immune system is through activation of lymphocytes to proliferate the initiation of mitosis via chemical mediators known as a mitogen. Lymphocytes, which comprised most of total white blood cells, acts as primary component responsible of various immunological responses [51]. Mitogen is mostly made up of bacteria and plants as carbohydrate-binding lectins [52]. Leucocyte proliferation, also defined as mitogenesis, begins after exposure to mitogens, such as concanavalin A (ConA) and phytohemagglutinin A (PHA), which primarily stimulate T-cells. At the same time, lipopolysaccharide (LPS) activates B-cells, and mitogenic pokeweed (PWM) can enhance both T- and B-cells. The main target of mitogens is the plasma membrane, whereby the mitogens attach to the carbohydrate substituents of membrane glycoproteins. For example, ConA attaches to α-D-mannosyl, while PWM and PHA bind to *N*-acetyl-D-glucosamine. The interaction with mitogen develops membrane receptors to stimulate adenylate cyclase, resulting in signal transduction from the membrane to the lymphocyte nucleus [53]. *In vitro* lymphocyte activation by respective mitogens enables the cells to generate specific immune response cytokines [54, 55]. The evaluation of proliferation can be determined easily by counting the growth in cell density, using a haemacytometer,

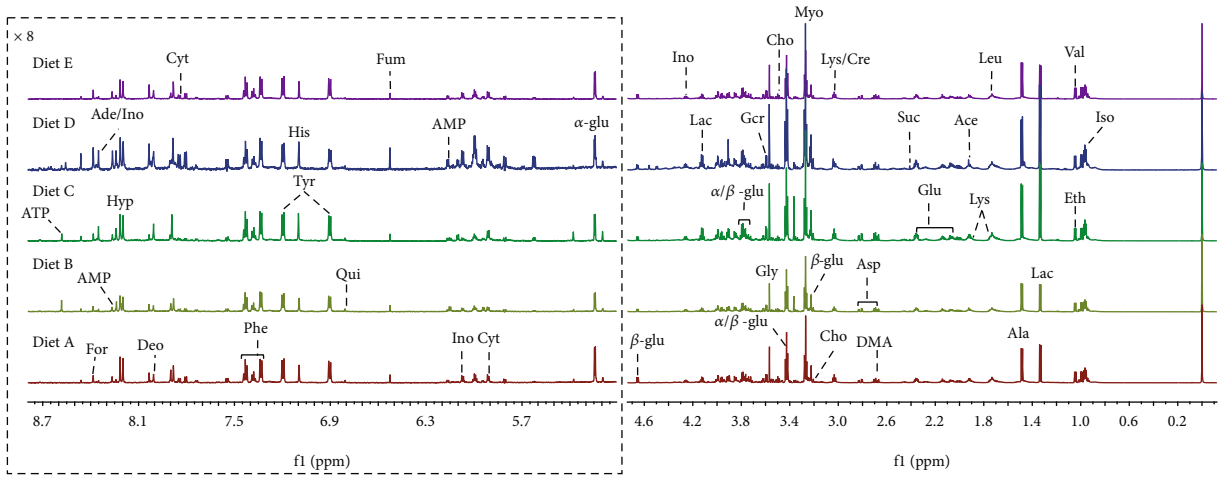

FIGURE 4: Representatives 700 MHz water-suppressed ^{1}H NMR spectra (0.5–9.0 ppm) of red hybrid tilapia spleen obtained from each of IG-supplemented diets (diets A, B, C, D and E). Abbreviations: Iso: isoleucine; Val: valine; Eth: ethanol; Lac: lactate; Ala: alanine; Leu: Leucine; Lys: lysine; Ace: acetate; Glu: glutamate; Suc: succinate; DMA: dimethylamine; Asp: aspartate; Cho: choline; α-, β-Glc: α-, β-glucose; m-I: myo-inositol; Gcr: glycerol; Gly: glycine; Ino: inosine; Cyt: cytidine; AMP: adenosine monophosphate; Fum: fumarate; Qui: quinone; Tyr: tyrosine; His: histidine; Phe: phenylalanine; Deo: deoxyguanosine; Hyp: hypoxanthine; ATP: adenosine triphosphate.

or more advanced techniques to measure the absorption of radiolabelled DNA precursors 3H-thymidine [56]. Thus, lymphoproliferation assay has become a critical parameter to evaluate the efficacy of dietary supplementation on immune response as it has been applied in numerous studies on tilapia [57–59].

Figure 3(a) demonstrates the number of T-cells stimulated by mitogen PHA and without mitogen calculated manually using a haemacytometer after 48 hours incubation. Diet C shows the highest number of cells with a clear stimulatory effect on leukocyte proliferation ($P \leq 0.05$) in the presence of mitogen in 8-fold accretion, followed by diets D (7-fold) and E (5-fold) compared to non-supplemented fish (diet A: control). Similarly, the highest number of B-cells stimulated by LPS was observed in diet C, followed by diet D significantly ($P < 0.05$) with fold change enhancement of 0.36 and 0.35, respectively, compared to control (Figure 3(b)). Interestingly, spontaneous lymphocyte proliferation in the absence of mitogens indicated a high proliferation of T- and B-cells but not significantly different from mitogen-stimulated proliferation.

This finding is in agreement with previous studies that demonstrated the immunomodulatory properties of several microalgae. For example, Chuang et al. [60] revealed that microalgae *Dunaliella salina* in 369 and 922.5 mg/kg doses has enhanced the significant proliferation of both T- and B-cells under untreated and LPS conditions ($P < 0.001$) after orally administered to leukemic mice. Based on the increment of T- and B-cells, it is believed that the actions of *D. salina* in leukemic mice might be involved in triggering a cascade of cellular and humoral immune responses. In another study, astaxanthin, a common carotenoid present in microalgae, had successfully stimulated mitogen-induced lymphoproliferation in humans. The stimulation index of T- and B-cells from peripheral blood mononuclear cells was consistently higher ($P < 0.05$) after being treated with dietary astaxanthin for eight weeks [61]. The administration of chrysophanic acid diet at 8 mg was also shown to significantly enhance the lymphocyte proliferation index in Indian major carps after 4 weeks of treatment; however, the index started to reduce after 8 weeks of feeding [62]. Therefore, this present finding could also be seen to prove the potential of IG as one of the promising candidates in boosting the innate and adaptive immune responses in red hybrid tilapia after 2 weeks of feeding.

3.4. Metabolite Profiles of the Spleen (1D and 2D NMR). Representative spleen spectra evaluated by 700 MHz ^{1}H NMR were labelled with identified metabolites acquired after 14 days treatment from each of IG-supplemented diets (diets A, B, C, D, and E) and are shown in Figure 4. The metabolite assignments were made based on 1D NMR chemical shift comparison with previous literature and matched with open access metabolomics databases such as the Human Metabolome Database (HMDB, http://www.hmdb.ca), and subsequently verified by 2D J-resolved and two-dimensional HSQC analysis. A total of 34 metabolites were successfully identified and listed in Table 1. Twenty-two metabolites were detected in the up to middle-field region (0.3–5.5 ppm) of the spectrum comprising overlapping signals of amino acids and carbohydrates with different intensities.

Meanwhile, in the downfield region of the spectrum (6.0–9.0 ppm), 13 metabolites were successfully detected, consisting of different types of nucleosides and amino acids mostly associated with an aromatic ring. Most of the assignments were made based on metabolites reported in a spleen sample from a rat model acquired on an NMR Bruker-AV600 spectrometer [63], except for leucine which was referred to De Pascali et al. [64]. Additional data provided by the ^{1}H-^{13}C HSQC correlation improved the identification of assigned metabolites but was limited to several compounds due to their low concentrations.

Identification of 8 compounds (**a** to **h**) was confirmed based on 2D-NMR of HSQC as shown in Figure 5.

Table 1: Chemical shift (ppm) and assignment of metabolite resonances in the spectrum of the spleen (s: singlet; d: doublet; t: triplet; dd: doublet of doublets; q: quartet; m: multiplet; ∗- undetermined J value due to condensed overlapping).

No	Tentative metabolite	δH (ppm), multiplicity, J (Hz)	HSQC
1.	Isoleucine	0.94 (t)∗ 1.02 (d)∗	13.93
2.	Leucine	0.96 (d, 7.4) 0.97 (d, 6.4) 1.70 (m)	23.70 24.84
3.	Valine	0.99 (d, 7.0) 1.05 (d, 7.0) 2.28 (m)	19.46 20.77
4.	Ethanol	1.19 (t, 7.0) 3.66 (q)∗	
5.	Lactate	1.34 (d, 6.8) 4.12 (q)∗	22.62
6.	Alanine	1.49 (d, 7.3) 3.77 (q)∗	19.08
7.	Lysine	1.73 (m) 1.90 (m) 3.03 (t, 8.8)	29.26
8.	Acetate	1.93 (s)	30.45
9.	Glutamate	2.07 (m) 2.14 (dd)∗ 2.36 (m)	29.88
10.	Succinate	2.41 (s)	
11.	Aspartate	2.69 (dd, 17.4, 8.7) 2.82 (dd, 17.4, 3.7) 3.91 (dd, 8.3, 4.2)	39.45 39.45
12.	Dimethylamine (DMA)	2.72 (s)	
13.	Creatine	3.04 (s) 3.94 (s)	
14.	Choline	3.21 (s) 3.51 (t, 9.3) 4.08 (m)	79.61
15.	β-Glucose	3.23 (t, 3.5) 3.43 (t, 6.6) 3.47 (dd, 5.8, 2.1) 3.74 (dd, 7.4, 4.8) 3.91 (dd, 8.3, 4.2) 4.66 (d, 8.1)	56.80 38.34 78.95 67.56
	Betaine	3.27 (s) 3.91 (s)	56.19 63.70
16.	Taurine	3.27 (t, 6.6) 3.43 (t, 6.6)	50.47
17.	Myo-inositol	3.27 (t, 6.6) 3.54 (dd, 9.8, 3.7) 3.63 (t)∗ 4.07 (t)∗	
18.	α-Glucose	3.43 (t, 6.6) 3.54 (dd, 9.8, 3.7) 3.75 (dd, 10.2, 4.4) 3.84 (m) 5.24 (d, 3.8)	39.03
19.	Glycine	3.57 (s)	
20.	Glycerol		

Table 1: Continued.

No	Tentative metabolite	δH (ppm), multiplicity, J (Hz)	HSQC
		3.59 (d, 5.1) 3.62 (d, 4.1) 3.79 (d, 7.3)	
21.	Serine	3.84 (m) 3.95 (m)	
22.	Adenosine monophosphate (AMP)	4.01 (dd, 8.1, 4.0) 4.32 (m) 4.53 (m) 6.16 (d, 5.9) 8.27 (s)	63.05
23.	Inosine	4.27 (m) 6.11 (d)∗ 8.24 (s) 8.35 (s)	68.90
24.	Cytidine	5.91 (d, 7.9) 6.07 (d, 7.3) 7.85 (d, 7.9)	
25.	Adenosine	6.07 (d, 7.3) 8.35 (s)	
26.	Fumarate	6.53 (s)	
27.	Quinone	6.81 (s)	
28.	Tyrosine	6.91 (d, 8.0) 7.20 (d, 8.2)	
29.	Histidine	7.10 (s) 8.01 (s)	
30.	Phenylalanine	7.33 (d, 7.5) 7.38 (t)∗ 7.43 (t, 7.6)	
31.	Deoxyguanosine	8.01 (s)	
32.	Hypoxanthine	8.19 (s), 8.21 (s)	
33.	Formate	8.46 (s)	
34.	Adenosine triphosphate (ATP)	8.58 (s)	

Isoleucine (**a**) was confirmed by the triplet peak detected at 0.94 ppm and cross-peaked to C-4 of the terminal methyl proton at 13.93 ppm. The cross-peaks of two doublets at 23.7 and 24.9 ppm in the HSQC spectra have verified the presence of terminal methyl protons of leucine (**b**). Valine (**c**) was confirmed from the correlation of its doublet at 1.05 ppm to 20.77 ppm, which is one of its terminal methyl carbons (CH_3). Meanwhile, the presence of glutamate was confirmed based on the correlation of the multiplet signal seen at 2.07 ppm with its methylene carbon (CH_2) at 29.88 ppm. The contrast between α- and β-glucose could be differentiated by the position of the anomeric hydrogens or the hydroxyl group attached to the anomeric carbon [65]. In the present study, β-glucose could be characterized by the appearance of a doublet at 4.66 ppm; meanwhile, α-glucose can be recognized by its doublet at 5.24 ppm. Unfortunately, no signal could be observed in the HSQC spectra probably due to its minute peak intensity. Taurine (**e**) was justified with the HSQC correlation of its triplet at 3.27 ppm with its methylene carbon (CH_2) at 50.47 ppm. Another metabolite is betaine (**f**) that was confirmed through the cross-peak of its singlet at 3.27 ppm and of the terminal methyl (CH_3) at 56.19 ppm (Figure 5).

Meanwhile, the downfield region of the spectra (6.0–9.0 ppm) shows the presence of adenosine monophosphate (AMP: g) that was confirmed when its doublet of doublet peak at 4.01 ppm correlated to one of methylene carbon (CH_2) at 63.05 ppm. AMP contains a purine skeleton connected to a ribose by monophosphate. The last confirmed metabolite through 2D HSQC correlation is inosine (h) which was assigned based on the correlation of the small doublet of doublet signal at 4.27 ppm with methine carbon (CH) at 68.90 ppm. However, the signal hardly could be seen in Figure 5. Inosine relates to a family of purine nucleosides made up of a ribosyl or deoxyribosyl moiety attached to a purine skeleton. Other metabolites were not identified using HSQC correlation due to their poor signals in the 1D NMR spectra. Nevertheless, their presence was confirmed by 2D JRES spectra of their multiplicity.

3.5. Metabolite Changes in Different Fish Group Diets. As an unsupervised and nonbiased method of class separation, the

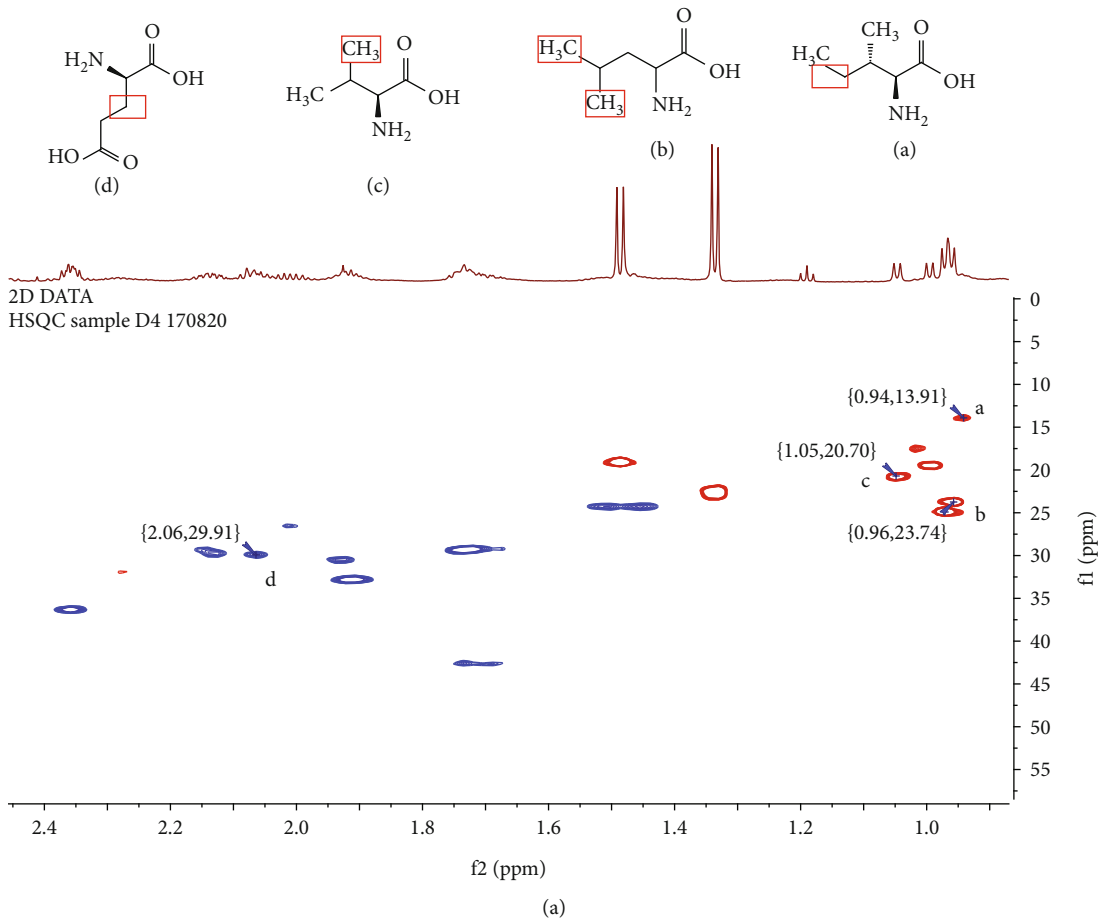

Figure 5: Continued.

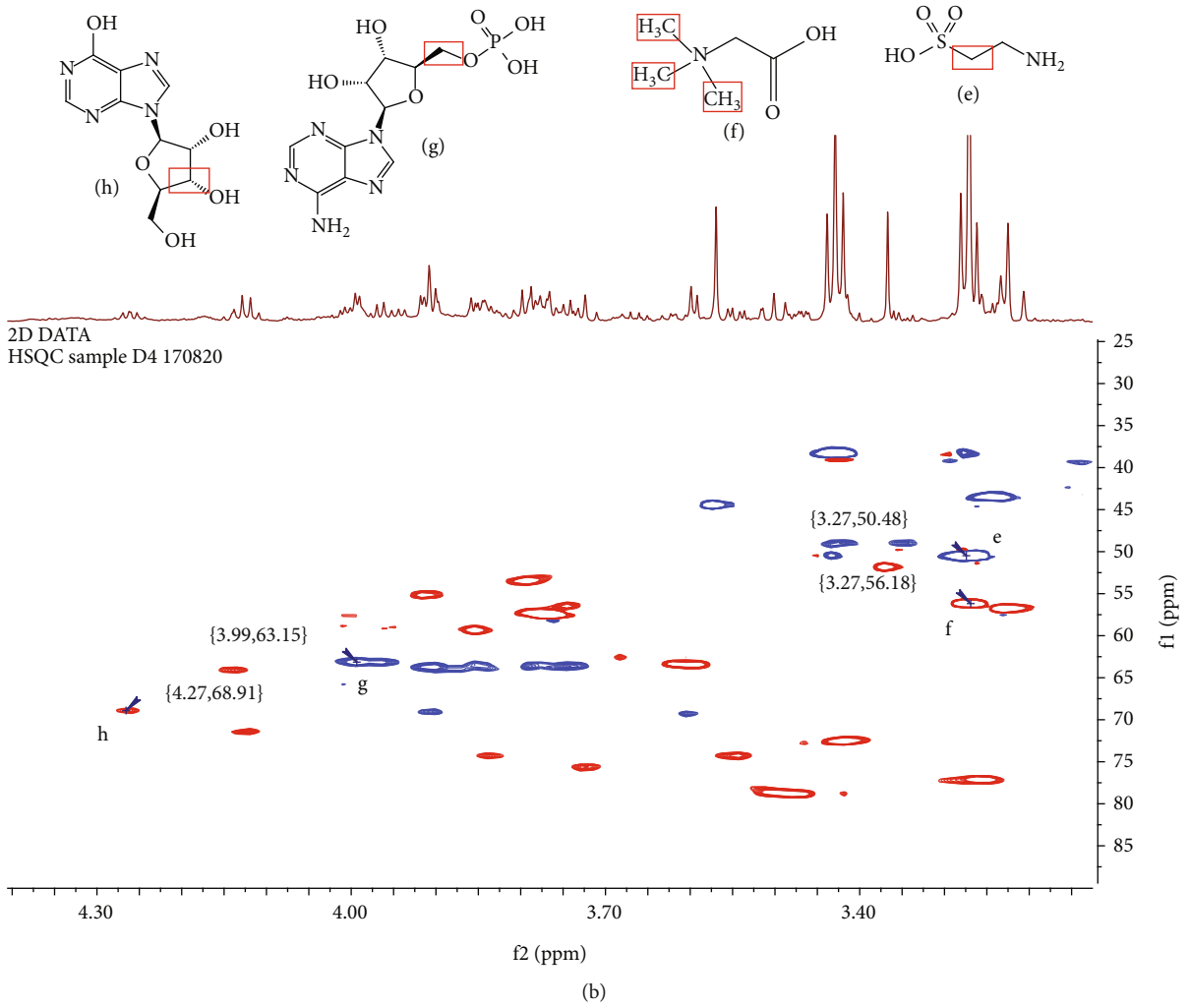

Figure 5: HSQC spectrum of fish spleen in the region (a) 0.80 to 2.40 ppm and (b) 3.20 to 4.30 ppm. The cross-peak signals were assigned as follows: (a) isoleucine; (b) leucine; (c), valine; (d) glutamate; (e) taurine; (f) betaine; (g) AMP, and (h) inosine.

primary purpose of PCA is to acquire preliminary information on the dataset without relying on any previous information referring to the data distribution. The prominent feature of PCA is that the differences are exposed, and thus, it is possible to measure the accuracy of the results, as it is not available in supervised methods. Therefore, supervised classification approaches (PLS-DA/OPLS-DA) guided by the appropriate PCA cluster are preferable for obtaining satisfactory biological outcomes [66].

The metabolite changes experienced after 14 days feeding regime of IG-supplemented diets in fish were observed through the PCA analysis on spleen ^{1}H-NMR data. The goodness of fit and predictability of the model showed four components with R2X value of 0.723 and Q2X value of 0.341. It is normal to obtain lower R2 and Q2 values in a biological model as shown in other fish metabolomics studies [67, 68]. The first two main components of PC1 and PC2 contributed 31.2% and 22.6%, describing a total of 54% of the variance. Each dot in the score plot (Figure 6(a)) defines as a spleen sample from a fish.

The score plot displays three clusters with group C and control group (diet A) were clustered together indicating both groups shared close similarity in chemical profiles. The IG-supplemented groups D and E, particularly E, were discriminated away from the control group, indicating their different metabolite content. However, no clear cluster was observed for B as its variables were scattered between two quadrants by PC1 due to a high intravariation. These clusters suggested that the fish in groups B, D, and E have experienced some metabolite changes causing them to move away from the control group (A).

The metabolites responsible for the separation are displayed in the loading plot (Figure 6(b)) wherein defined by variables with respective bins of NMR chemical shift regions with acceptable 95% jack and knife bars. The variables assigned as betaine, taurine, choline, and α- and β-glucose located on the positive side of PC1 were more prominent in group C and control. In contrast, metabolites on the negative side of PC1 were identified as leucine, isoleucine, and lysine presented higher in group E. Glutamate, serine, glycine, and aspartate were dominated in diet D, on the positive side of PC2.

3.6. Biomarker Identification Using OPLS Model. The potential biomarkers for the immunomodulatory effects of IG

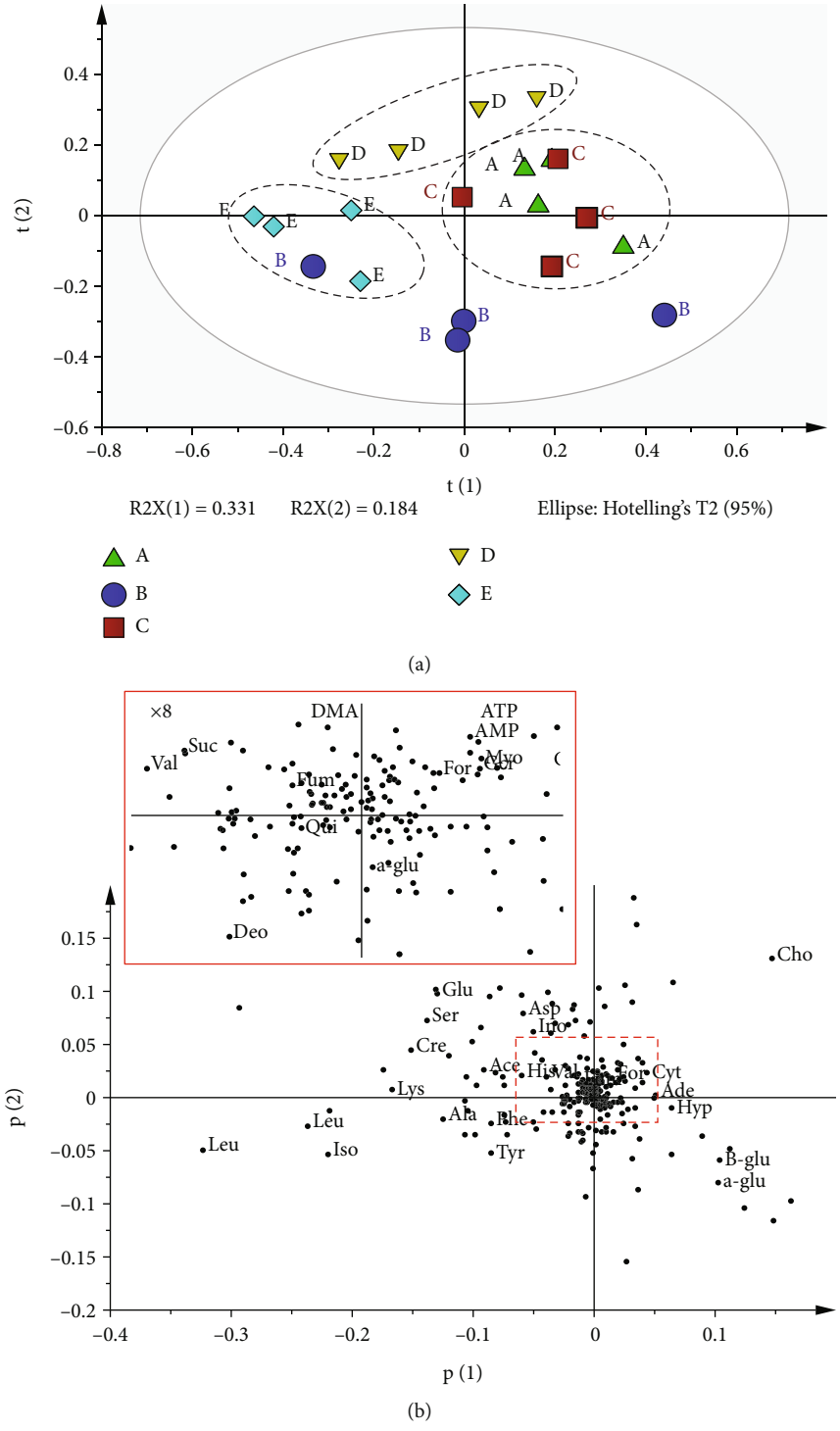

Figure 6: PCA score plot (a) and (b) loading scatter plot on ^{1}H NMR spectra of fish fed diets containing different IG contents (A: 0.0%, B: 0.6%, C: 1.3%, D: 2.5%, and E: 5.0%) (Abbreviations: Iso: isoleucine; Val: valine; Eth: ethanol; Lac: lactate; Ala: alanine; Leu: Leucine; Lys: lysine; Ace: acetate; Glu: glutamate; Suc: succinate; DMA: dimethylamine; Asp: aspartate; Cho: choline; α-, β-Glc: α-, β-glucose; m-I: myo-inositol; Gcr: glycerol; Gly: glycine; Ino: inosine; Cyt: cytidine; AMP: adenosine monophosphate; Fum: fumarate; Qui: quinone; Tyr: tyrosine; His: histidine; Phe: phenylalanine; Deo: deoxyguanosine; Hyp: hypoxanthine; ATP: adenosine triphosphate).

were further analyzed using a supervised OPLS model to correlate between metabolites in the spleen and the conducted immunomodulatory bioactivities (phagocytosis, RBA, and lymphoproliferation). The respective model was generated between ^{1}H NMR data of diet A as control and diet D (2.5% IG), as displayed in Figure 7(a) since this group consistently gives significant results among the conducted bioactivities. Four components were generated (Figure 7(b)) with acceptable goodness of fit and predictability as represented by values of R2Y = 0.88 and Q2Y = 0.60

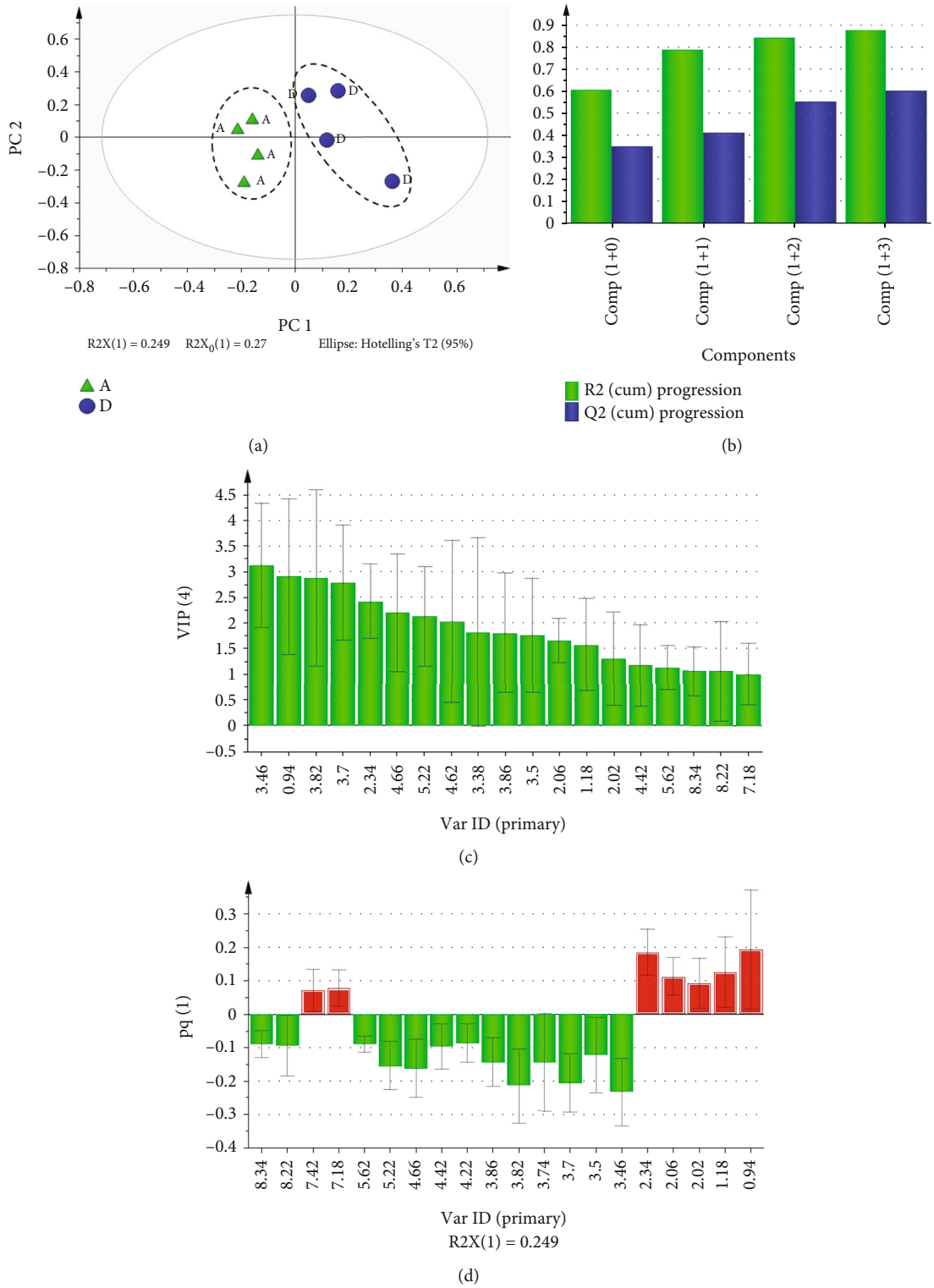

Figure 7: OPLS model between diet A and D. (a) Score plot between diet A and diet D. (b) Summary of fit generated. (c) VIP plot with value more than 1. (d) Loading column plot representing a list of sorted variables contributed to diet A (green columns) and diet D (red columns).

with a difference between them not more than 0.3 [69]. Hundred random permutations of the y-variable conducted for each bioactivity verified the minimum validity of the current model after y-axis intercepts below zero as stated in SIMCA. However, the validity of each bioactivity was supported with observed vs predicted plots with excellent correlation between all bioactivities (Y-data) and metabolites (X-data) represented by regression lines with a value between 0.74 and 0.97. Their permutation tests and observed vs predicted plots are provided in Figures 8 and 9.

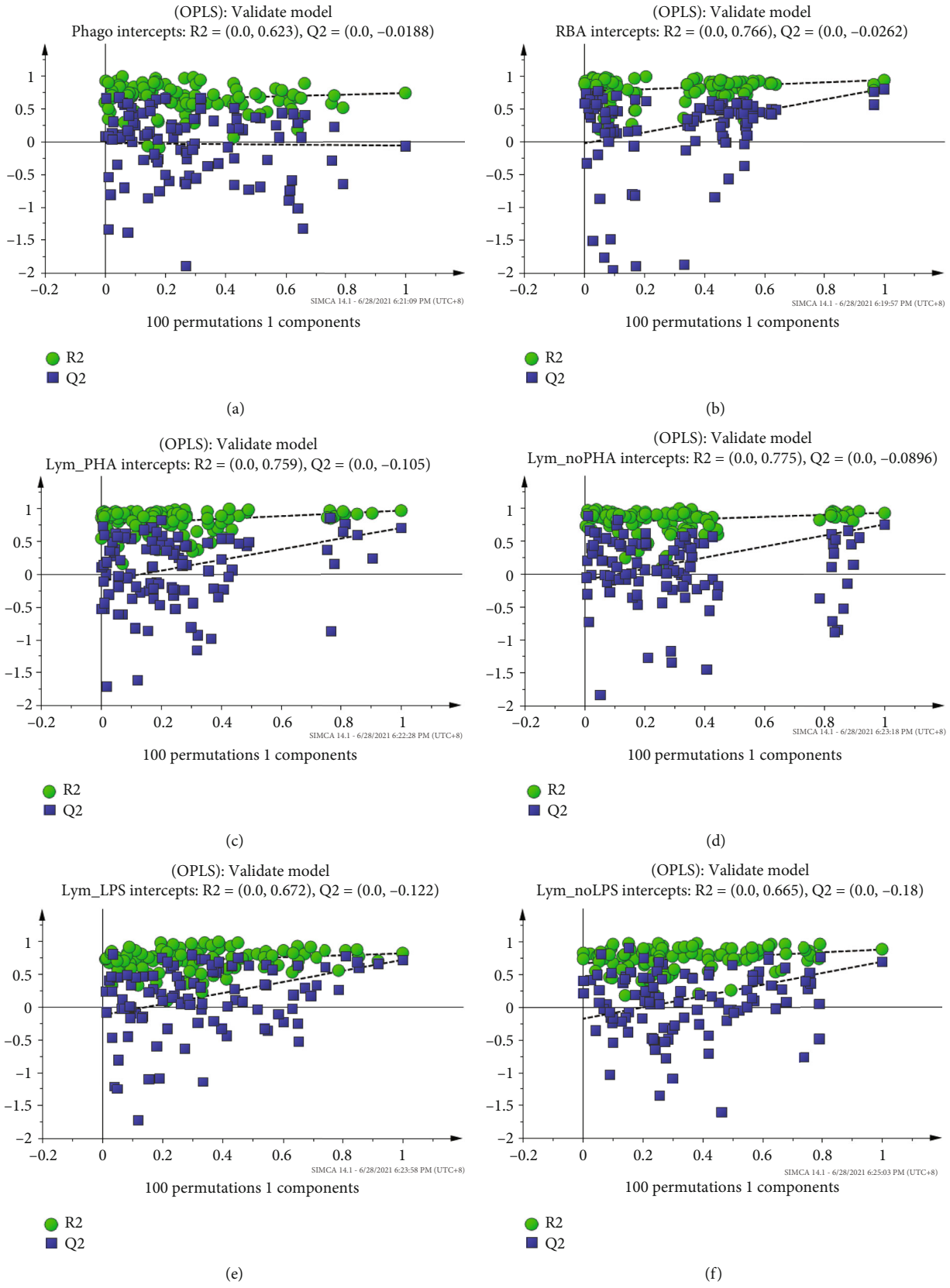

Figure 8: Hundred permutation test plots for each of the bioactivities included in OPLS model. (a) Phagocytosis activities. (b) Respiratory burst activity. (c) Lymphoproliferation with mitogen PHA. (d) Lymphoproliferation without mitogen PHA. (e) Lymphoproliferation with mitogen LPS. (f) Lymphoproliferation without mitogen LPS.

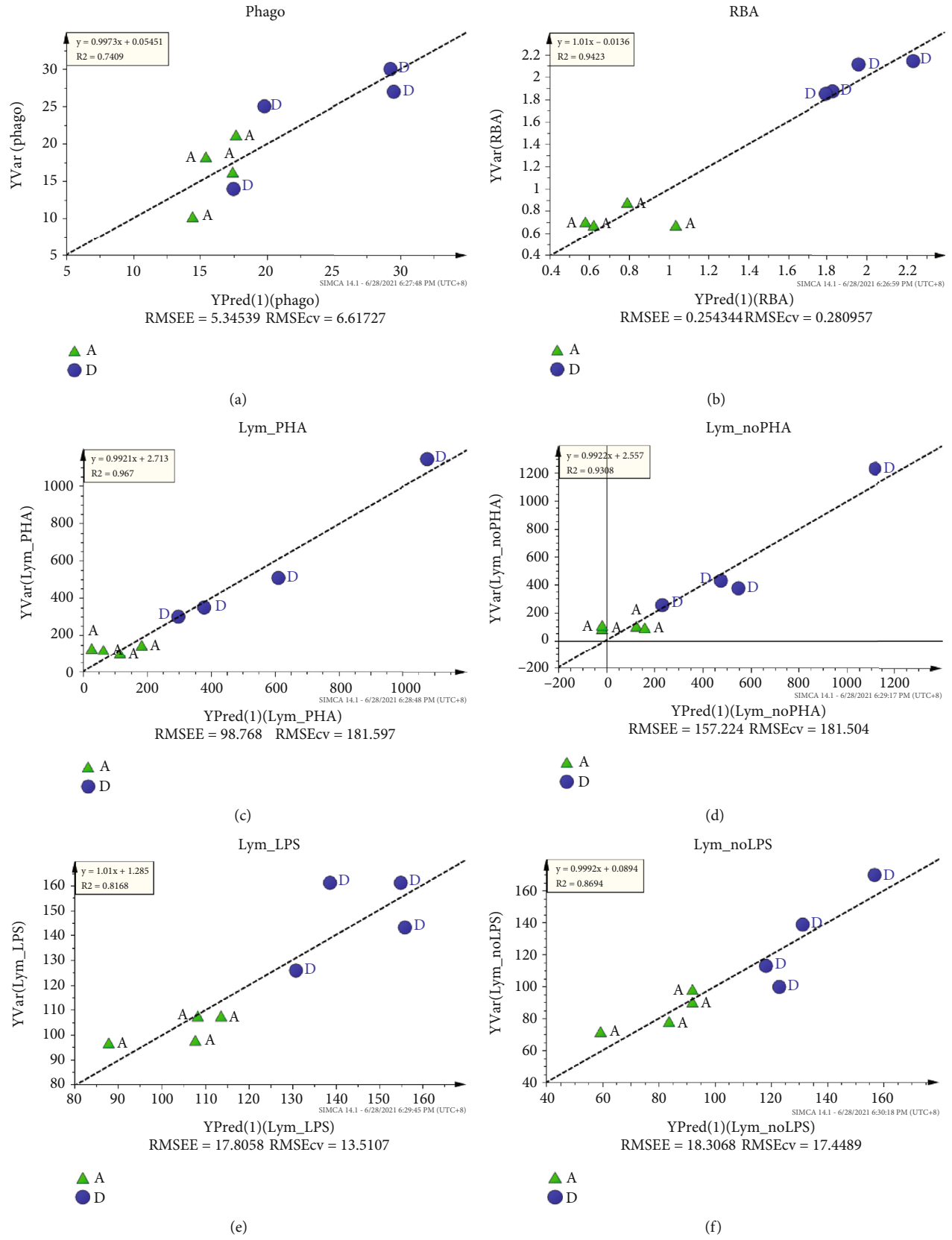

Figure 9: Observed vs predicted plot for each of the bioactivities included in PLS model. (a) Phagocytosis activities. (b) Respiratory burst activity. (c) Lymphoproliferation with mitogen PHA. (d) Lymphoproliferation without mitogen PHA. (e) Lymphoproliferation with mitogen LPS. (f) Lymphoproliferation without mitogen LPS.

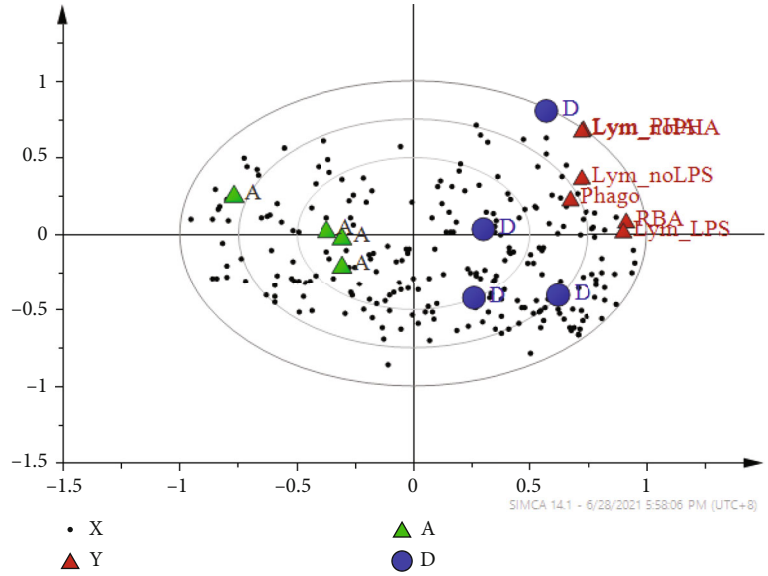

Figure 10: The bi-plot of OPLS model representing the correlation between metabolites obtained from ^{1}H NMR analysis in diet A and diet D with the biological activities (RBA: respiratory burst activities, Phago: phagocytosis activities, Lym PHA: lymphoproliferation with mitogen PHA, Lym no PHA: lymphoproliferation without mitogen PHA, Lym LPS: lymphoproliferation with mitogen LPS, Lym no LPS: lymphoproliferation without mitogen LPS).

The significance of any variable was determined by analyzing the variable importance in a projection (VIP) plot with jack-knifing uncertainty bars. The variables with VIP scores of more than 1 with the error bar not crossing the baseline in the loading column plot were retained as significant. The selected bars could be classified as chemical markers or biomarkers as depicted in Figure 7(c) with separation by PC1 between groups A and D. Six of them on the positive side in red column were upregulated and belong to diet D, and thirteen downregulated metabolites are on the negative side in green column for diet A (Figure 7(d)). These variables were identified as corresponding potential biomarkers by comparing their variable IDs with a list of identified chemical shifts in NMR spectra based on the previous literature and open access metabolomics database and subsequently verified by 2D J-resolved and HSQC analysis.

The relationship of the variables between their distribution in the score plot and separation in the loading plots was summarized in a biplot as shown in Figure 10. The biplot of the OPLS model discriminated diet A (control) from D (2.5% IG) with all bioactivities of phagocytosis, respiratory burst activity, and lymphoproliferation was clustered together with diet D. The variables were identified as isoleucine, glutamate, ethanol, and tyrosine which upregulated in the IG-supplemented (D) tested groups compared to the control (A). The other 13 variables such as glucose, choline, inosine, and adenosine were downregulated in the control group compared to the IG-supplemented group.

3.6.1. Upregulated Metabolism. There are four metabolites significantly upregulated in the 2.5% IG-supplemented group (diet D): isoleucine, glutamate, ethanol, and tyrosine, involved in a few metabolic pathways suggested by the Kyoto Encyclopedia of Genes and Genomes (KEGG), as shown in Table 2. The most important upregulated metabolite in D based on VI*P* value is isoleucine, with a significant fold change value compared to the control group. Isoleucine is an essential branched-chain amino acid that fishes obtain from an external diet to fulfil certain biochemical reactions and growth requirements. It includes lipolysis, lipogenesis, glucose metabolism, glucose transportation, intestinal amino acid transport, benefiting embryo growth, and immunity [70]. It has been discovered that isoleucine deficiency in the diet leads to biochemical malfunctions including growth interruption [71, 72]. In the present study, isoleucine is one of the metabolites with a significant increment in fish spleen cells after being fed with an IG-supplemented diet when compared to the commercial diet. The isoleucine increase could be related to its presence with other amino acids in IG which successfully identified via NMR in polar solvents as reported before [73]. A recent study found isoleucine enhanced growth performance and intestinal immunology of hybrid catfish. After eight weeks of dietary isoleucine (12.5 g/kg diet), the activities of lysozyme, acid phosphatase, and alkaline phosphatase, and the contents of complement 3 (*C3*), *C4*, and immunoglobulin M (*IgM*) significantly increased [74]. In a different study, dietary isoleucine up to 16 g/kg intake by fingerling *Channa punctatus* for 12 weeks has significantly improved serum protein, lysozyme, and superoxide dismutase activities, improved growth and haematological parameters [75]. Superoxide dismutase (SOD) is an essential component of the enzyme mechanism and protects cells from the harmful effects of endogenic superoxide radicals [76, 77]. SOD activates the transformation of radical superoxide into hydrogen peroxide and molecular oxygen. ROS formation in fish could be influenced by

Table 2: ^{1}H NMR signal assignment for potential biomarkers derived from OPLS model of 2.5% IG-supplemented diet against control, their fold change values, and associated metabolic pathways (∗ = $P < 0.05$ vs control).

Metabolites	Chemical shift (ppm)	VIP value	Fold change	Metabolic pathway
Upregulated				
Isoleucine	0.94	2.91	1.44∗	Valine, leucine, and isoleucine biosynthesis
Glutamate	2.34	2.42	1.50∗	D-glutamine and D-glutamate metabolism
Ethanol	1.18	1.58	1.72	Glycolysis
Tyrosine	7.18	1.01	1.51∗	Tyrosine metabolism
Downregulated				
α/β-Glucose	3.46	3.13	0.61∗	Glycolysis/gluconeogenesis
Unknown	3.70	2.79	0.66∗	—
Choline	3.50	1.76	0.84	Glycine, serine, and threonine metabolism
Inosine	4.42	1.17	0.88	Purine metabolism
Hypoxanthine	8.22	1.07	0.58	Purine metabolism
Adenosine	8.34	1.07	0.61	Purine metabolism

isoleucine. The elimination of ROS in fish is accomplished through antioxidant protection and seems to be primarily dependent on antioxidant compounds such as glutathione (GSH) and antioxidant enzymes. The improvement of O^{-2} and ·OH-scavenging ability can be seen in an isoleucine-incorporated diet. In addition, sufficient isoleucine (6.6–12.5 g/kg diet) could enhance the elimination of free radicals by minimizing the oxidative damage in fish muscle mainly through the NF-E2-related factor 2 (*Nrf2*) signalling pathway [78].

Another significantly upregulated metabolite of the IG-supplemented diet is glutamate, which was identified based on three different chemical shifts at 2.34, 2.06, and 2.02 ppm with a significant fold change value compared to the commercial diet (Table 2). As one of the nonessential amino acids, L-Glutamate is a functional amino acid present in both animal and plant proteins responsible for cell metabolism and signalling [79, 80]. Glutamate is also an important energy source in the small intestine [81], and a precursor of essential compounds such as glutathione (GSH) [82]. In the past fish research, glutamate dietary dissolved in Dulbecco's Modified Eagle Medium (DMEM) has been proven to enhance the antioxidant ability and modulate the antioxidant-related signalling molecule expression in the intestine as well as in enterocytes [83, 84]. This study suggests the biosynthesis of glutamate that probably originated from α-ketoglutarate [85]. The reversible reactions involved in converting α-ketoglutarate to glutamate catalyzed by glutamate dehydrogenase as illustrated in Figure 11. Recent studies have found dietary glutamate in certain fish species with improved growth efficiency and immune responses. For instance, low-phosphorus diet supplementation of 10 g/kg glutamate boosted the behaviour of intestinal antioxidant enzymes and enhanced the immune system of juvenile mirror carp [86].

Ethanol was also found to be enhanced in the IG-supplemented diet. However, the increment measured was not significant, probably due to high variations between replicates. The increment of ethanol could be associated with glycolysis due to high glucose content in IG as reported previously in the relative quantification of metabolites identified [73]. Previous studies have proven the impact of ethanol on immunomodulatory properties [87, 88].

3.6.2. Downregulated Metabolism. In the present study, IG supplementation led to the lower concentration of α/β-glucose, choline, inosine, hypoxanthine, adenosine, and unknown as simplified in Table 2. These changes could be correlated with perturbations in glycolysis/gluconeogenesis; purine metabolism; glycine, serine, and threonine metabolism. The most downregulated with the highest VIP value metabolites were α/β-glucose which involved in glycolysis/gluconeogenesis as suggested by KEGG. Their concentrations were both 0.61 folds decreased (Figure 11). Glucose is an essential fuel for ATP production to fulfil the bioenergetic requirements of the cell. The first phase of glycolysis requires the phosphorylation of glucose via hexokinase to create glucose-6-phosphate (G6P). The mechanism then continues as a sequence of enzymatic reactions that eventually generate pyruvate. Pyruvate may have several fates in the cell-based cellular function, one of which is oxidized to CO_2 inside mitochondria for the optimized yield of ATP. During aerobic glycolysis, pyruvate is also transformed to lactate, a metabolic product adopted by cells that participated in vigorous growth and multiplication [89]. Glycolysis modulation is an important step in activating innate and adaptive immune cells. It provides a way to generate macromolecules and trigger the antimicrobial respiratory burst through flux enrichment in the pentose phosphate pathway [17]. During 18 hours after immune stimulation, T-cells regulate their metabolic processes, enhancing the release of glucose transporters and glycolytic enzymes. T-cells then trigger aerobic glycolysis in preparation for the activation of extensive clonal growth [90]. Therefore, a sufficient source of glucose is necessary for the sustainability of high glycolysis levels. The biplot of the OPLS model (Figure 8) depicts all biological

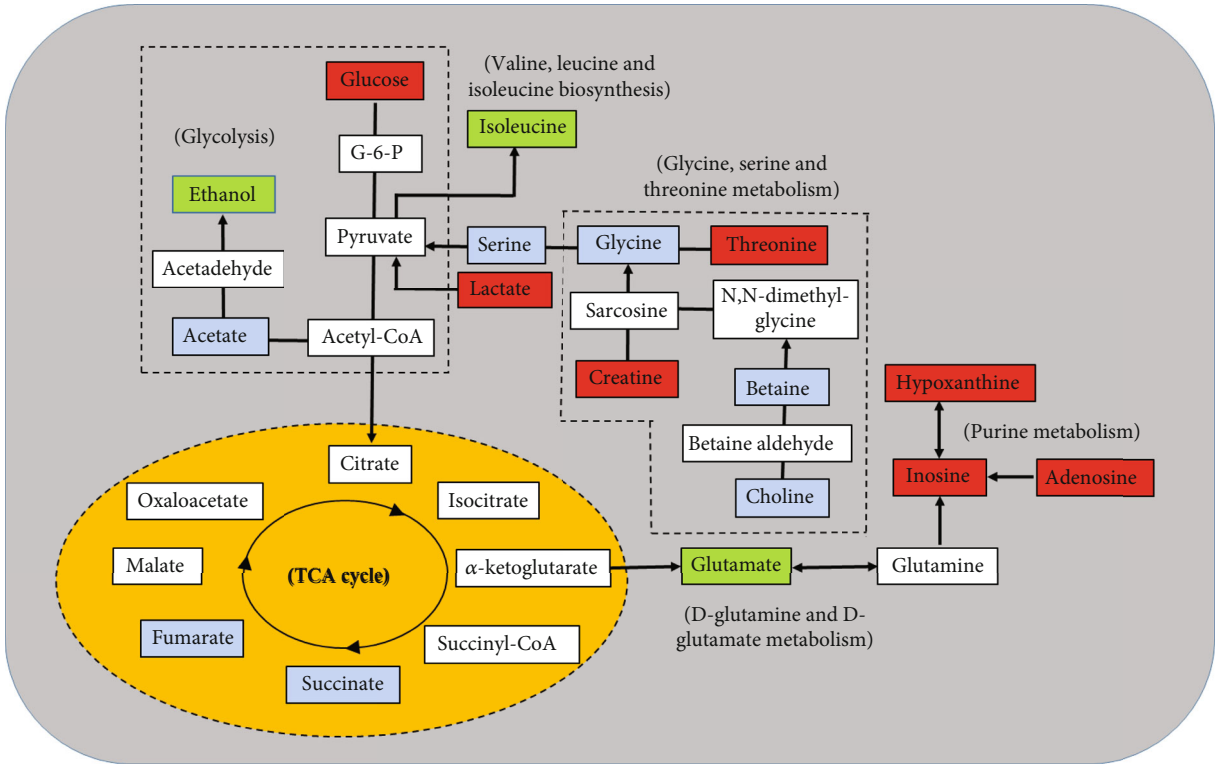

Figure 11: Proposed metabolic pathways affected by IG-supplemented diet as detected in the spleen of red hybrid tilapia (metabolites in green and red boxes represent up-regulated and down-regulated levels, respectively, in IG-supplemented group compared with the control group. Metabolites in blue and white boxes respectively represent those detected and not detected during analysis).

activities being discriminated against together with the IG supplementation diet (diet D) due to the high glucose content which has provided more energy for the glycolysis pathway compared to the control group (diet A).

Table 2 shows the hypoxanthine, adenosine, and inosine levels in the IG supplementation group have decreased up to 0.58, 0.61, and 0.88 folds, respectively. These three purine nucleotides involve in the purine metabolism pathway, as suggested by KEGG. Purines are the most abundant metabolites in all biological entities as they are a key source for DNA and RNA building blocks. Apart from that, purines contribute as a fuel source and cofactor to support cell growth and replication. Purines and their components are also normally involved in biochemical mechanisms, including immune functions and host-tumour interactions [91]. The metabolism of purines is defined as the biochemical pathway of building and breaking down the purines inside an organism. This metabolism involves the biosynthetic process of de novo purine, the mechanism of purine salvage, and purine breakdown. The transformation of phosphoribosylpyrophosphate (PRPP) into inosine $5'$-monophosphate (IMP) occurs via the de novo purine biosynthetic pathway catalyzed by several enzymes. Meanwhile, purine salvage recycles hypoxanthine, inosine, and adenine as substrates to produce purine nucleotides. Inosine and hypoxanthine in the purine degradation pathway can be further oxidized into xanthine and uric acid [92]. Furthermore, the metabolite at 3.70 ppm remained unknown as its singlet peak could not be matched with any previously reported study or referred open access metabolomics databases.

4. Conclusions

The current study describes the first work in which a metabolic approach was used to analyze the red hybrid tilapia spleen cells administered with an IG-supplemented diet. Our findings revealed that IG supplementation at a concentration of 2.5% has enhanced the immune response of innate immunity, which may be beneficial for protecting the health condition of the fish. The OPLS analysis demonstrated that three significant metabolites, namely, tyrosine, glutamate, and isoleucine, were substantially upregulated in the 2.5% IG-supplemented (diet D) fish compared to the control group (diet A). The IG supplementation also resulted in lower concentrations of various metabolites in the spleen including α/β-glucose, choline, hypoxanthine, adenosine, and inosine, which are involved in glycolysis and purine degradation. The metabolite alterations in the red hybrid tilapia spleen reflect both the activity and immune response in fish, suggesting that IG supplementation has strongly influenced the metabolic condition in fish cells and further boosted the immune response and health status. These findings have also proved to be successful the application of metabolomics tools in the discovery of alternative healthy feed from microalgae species to improve fish health in meeting the aquaculture's future targets. However, further

investigation is required to explore the impact of IG supplementation on these biomarkers during microbial infections.

Data Availability

Data available on request.

Conflicts of Interest

The authors declare no conflict of interest.

Acknowledgments

We would also like to acknowledge Dr. Md. Shirajum Monir, Mr. Aslah Mohamad, and Mr. Muhammad Afiq Ngadni for the assistance given during the fish samples collection. A special thanks are due to Dr. Azira Muhamad from Malaysia Genome Institute for technical assistance during NMR analysis using Bruker 700 MHz. This research has been financially supported by Ministry of Higher Education Malaysia (MOHE) to Japan Science and Technology Agency (JST)/Japan International Cooperation Agency (JICA) through joint research program Science and Technology Research Partnership for Sustainable Development (SATREPS) in the project for Continuous Operation System for Microalgae Production Optimized for Sustainable Tropical Aquaculture (COSMOS) under research grant scheme 6300856-12038.

References

[1] FAO, *The Future of Food and Agriculture: Trends and Challenges*, Food and Agriculture Organization of the United Nations, Rome, Italy, 2017.

[2] DOF, *Annual Fisheries Statistics*, Department of Fisheries Malaysia, Ministry of Agriculture & Agro-Based Industry, Malaysia, 2020.

[3] M. G. Bondad-Reantaso, R. P. Subasinghe, J. R. Arthur et al., "Disease and health management in Asian aquaculture," *Veterinary Parasitology*, vol. 132, no. 3-4, pp. 249–272, 2005.

[4] E. D. Abarike, F. K. A. Kuebutornye, J. Jian, J. Tang, Y. Lu, and J. Cai, "Influences of immunostimulants on phagocytes in cultured fish: a mini review," *Reviews in Aquaculture*, vol. 11, no. 7, pp. 1–9, 2019.

[5] P. Elumalai, A. Kurian, S. Lakshmi, C. Faggio, M. A. Esteban, and E. Ringø, "Herbal immunomodulators in aquaculture," *Reviews in Fisheries Science and Aquaculture*, vol. 29, no. 1, pp. 33–57, 2021.

[6] G. Rashidian, J. T. Boldaji, S. Rainis, M. D. Prokić, and C. Faggio, "Oregano (*Origanum vulgare*) extract enhances zebrafish (*Danio rerio*) growth performance, serum and mucus innate immune responses and resistance against *Aeromonas hydrophila* challenge," *Animals*, vol. 11, no. 2, pp. 1–12, 2021.

[7] S. E. Fadl, M. S. Elgohary, A. Y. Elsadany, D. M. Gad, F. F. Hanaa, and N. M. El-habashi, "Contribution of microalgae-enriched fodder for the Nile tilapia to growth and resistance to infection with *Aeromonas hydrophila*," *Algal Research*, vol. 27, pp. 82–88, 2017.

[8] A. A. A. Galal, R. M. Reda, and A. A. Mohamed, "Influences of *Chlorella vulgaris* dietary supplementation on growth performance, hematology, immune response and disease resistance in *Oreochromis niloticus* exposed to sub-lethal concentrations of penoxsulam herbicide," *Fish and Shellfish Immunology*, vol. 77, pp. 445–456, 2018.

[9] N. HabashiEl, S. E. Fadl, H. F. Farag, D. M. Gad, A. Y. Elsadany, and M. S. El, "Effect of using spirulina and chlorella as feed additives for elevating immunity status of Nile tilapia experimentally infected with Aeromonas hydrophila," *Aquaculture Research*, vol. 50, no. 10, pp. 2769–2781, 2019.

[10] M. Devos, L. Poisson, F. Ergan, and G. Pencreac'h, "Enzymatic hydrolysis of phospholipids from *Isochrysis galbana* for docosahexaenoic acid enrichment," *Enzyme and Microbial Technology*, vol. 39, no. 4, pp. 548–554, 2006.

[11] Y. Lin, F. Chang, C. Tsao, and J. Y. Leu, "Influence of growth phase and nutrient source on fatty acid composition of *Isochrysis galbana* CCMP 1324 in a batch photoreactor," *Biochemical Engineering Journal*, vol. 37, no. 2, pp. 166–176, 2007.

[12] J. Liu, M. Sommerfeld, and Q. Hu, "Screening and characterization of isochrysis strains and optimization of culture conditions for docosahexaenoic acid production," *Applied Microbiology and Biotechnology*, vol. 97, no. 11, pp. 4785–4798, 2013.

[13] S. Babuskin, K. Radhakrishnan, P. A. S. Babu, M. Sivarajan, and M. Sukumar, "Effect of photoperiod, light intensity and carbon sources on biomass and lipid productivities of Isochrysis galbana," *Biotechnology Letters*, vol. 36, no. 8, pp. 1653–1660, 2014.

[14] A. P. Batista, L. Gouveia, N. M. Bandarra, J. M. Franco, and A. Raymundo, "Comparison of microalgal biomass profiles as novel functional ingredient for food products," *Algal Research*, vol. 2, no. 2, pp. 164–173, 2013.

[15] G. Di Lena, I. Casini, M. Lucarini, and G. Lombardi-Boccia, "Carotenoid profiling of five microalgae species from large-scale production," *Food Research International*, vol. 120, pp. 810–818, 2019.

[16] S. M. Kim, Y. Jung, O. Kwon et al., "A potential commercial source of fucoxanthin extracted from the microalga Phaeodactylum tricornutum," *Applied Biochemistry and Biotechnology*, vol. 166, no. 7, pp. 1843–1855, 2012.

[17] K. Ganeshan and A. Chawla, "Metabolic regulation of immune responses," *Annual Review of Immunology*, vol. 32, pp. 609–634, 2018.

[18] A. C. Alfaro and T. Young, "Showcasing metabolomic applications in aquaculture: a review," *Reviews in Aquaculture*, vol. 10, no. 1, pp. 135–152, 2018.

[19] L. M. Samuelsson and D. G. J. Larsson, "Contributions from metabolomics to fish research," *Molecular BioSystems*, vol. 4, no. 10, pp. 974–979, 2008.

[20] D.-D. Wei, J.-S. Wang, M.-H. Li et al., "A Pilot Study of the Onset of Hepatic Encephalopathy (OHE) in Mice Induced by Thioacetamide and the Protective Effect of Taurine by Holistic Metabolic Characterization," *Metabolomics*, vol. 11, pp. 559–570, 2014.

[21] J. Tompkins, M. DeVille, J. Day, and M. Turner, *Culture Collection of Algae and Protozoa: Catalogue of Strains*, Titus Wilson and Son Ltd., 1995.

[22] P. Lavens and P. Sorgeloos, "Manual on the production and use of live food for aquaculture," in *FAO fisheries technical paper no. 361*, FAO Rome, 1996.

[23] L. M. Aguilera-Sáez, A. C. Abreu, J. Camacho-Rodríguez, C. V. González-López, M. Del Carmen Cerón-García, and I. Fernández, "NMR metabolomics as an effective tool to

unravel the effect of light intensity and temperature on the composition of the marine microalgae Isochrysis galbana," *Journal of Agricultural and Food Chemistry*, vol. 67, no. 14, pp. 3879–3889, 2019.

[24] T. B. Schock, S. Newton, K. Brenkert, J. Leffler, and D. W. Bearden, "An NMR-based metabolomic assessment of cultured cobia health in response to dietary manipulation," *Food Chemistry*, vol. 133, no. 1, pp. 90–101, 2012.

[25] Q. Ai, K. Mai, L. Zhang et al., "Effects of dietary vitamin C on survival, growth, and immunity of large yellow croaker, *Pseudosciaena crocea*," *Aquaculture*, vol. 261, no. 1, pp. 327–336, 2006.

[26] C. Secombes, "Isolation of salmonid macrophages and analysis of their killing activity," in *Techniques in Fish Immunology*, J. Stolen, T. Fletcher, D. Anderson, B. Robertsen, and W. Muiswinkel, Eds., pp. 137–154, SOS Publications, 1990.

[27] N. Tian, J. S. Wang, P. R. Wang, X. F. Song, M. H. Yang, and L. Y. Kong, "NMR-based metabonomic study of Chinese medicine Gegen Qinlian Decoction as an effective treatment for type 2 diabetes in rats," *Metabolomics*, vol. 9, no. 6, pp. 1228–1242, 2013.

[28] L. Eriksson, J. Trygg, and S. Wold, "CV-ANOVA for significance testing of PLS and OPLS® models," *Journal of Chemometrics*, vol. 22, no. 11–12, pp. 594–600, 2008.

[29] T. Aoki, T. Takano, M. Santos, H. Kondo, and I. Hirono, "Molecular innate immunity in teleost fish: review and future perspectives: Fisheries for Global Welfare and Environment," in *Fisheries for Global Welfare and Environment, Memorial Book of the 5th World Fisheries Congress*, pp. 263–276, Terrapub, Tokyo, Japan, 2008.

[30] C. Uribe, H. Folch, R. Enriquez, and G. Moran, "Innate and adaptive immunity in teleost fish: a review," *Veterinari Medicina*, vol. 56, no. 10, pp. 486–503, 2011.

[31] I. Whang, Y. Lee, S. Lee et al., "Characterization and expression analysis of a goose-type lysozyme from the rock bream *Oplegnathus fasciatus*, and antimicrobial activity of its recombinant protein," *Fish and Shellfish Immunology*, vol. 30, no. 2, pp. 532–542, 2011.

[32] L. Grayfer, J. Hodgkinson, and M. Belosevic, "Antimicrobial responses of teleost phagocytes and innate immune evasion strategies of intracellular bacteria," *Developmental and Comparative Immunology*, vol. 43, no. 2, pp. 223–242, 2014.

[33] W. Sirimanapong, K. Thompson, K. Kledmanee et al., "Optimisation and standardisation of functional immune assays for striped catfish (*Pangasianodon hypophthalmus*) to compare their immune response to live and heat killed *Aeromonas hydrophila* as models of infection and vaccination," *Fish and Shellfish Immunology*, vol. 40, no. 2, pp. 374–383, 2014.

[34] D. Carbone and C. Faggio, "Importance of prebiotics in aquaculture as immunostimulants. Effects on immune system of *Sparus aurata* and *Dicentrarchus labrax*," *Fish and Shellfish Immunology*, vol. 54, pp. 172–178, 2016.

[35] A. Vazirzadeh, A. Marhamati, R. Rabiee, and C. Faggio, "Immunomodulation, antioxidant enhancement and immune genes up-regulation in rainbow trout (*Oncorhynchus mykiss*) fed on seaweeds included diets," *Fish and Shellfish Immunology*, vol. 106, pp. 852–858, 2020.

[36] H. M. Ragap, R. H. Khalil, H. H. Mutawie, H. M. Ragap, and R. H. Khalil, "Immunostimulant effects of dietary Spirulina platensis on tilapia Oreochromis niloticus," *Journal of Applied Pharmaceutical Science*, vol. 2, no. 2, pp. 26–31, 2012.

[37] R. Cerezuela, F. A. Guardiola, J. Meseguer, and M. Á. Esteban, "Enrichment of gilthead seabream (Sparus aurata L.) diet with microalgae: effects on the immune system," *Fish Physiology and Biochemistry*, vol. 38, no. 6, pp. 1729–1739, 2012.

[38] J. Chung, X. Ou, R. P. Kulkarni, and C. Yang, "Counting white blood cells from a blood smear using Fourier ptychographic microscopy," *PLoS One*, vol. 10, no. 7, pp. 1–10, 2015.

[39] J. D. Biller-Takahashi, L. S. Takahashi, F. P. Caunesp, and F. D. A. Sebasti, "Serum bactericidal activity as indicator of innate immunity in pacu Piaractus mesopotamicus (Holmberg, 1887)," *Arquivo Brasileiro de Medicina Veterinária e Zootecnia*, vol. 65, no. 6, pp. 1745–1751, 2013.

[40] A. Barreiros, J. David, and J. David, "Estresse Oxidativo: Relação Entre Geração de Espécies Reativas e Defesa Do Organismo," *Química Nova*, vol. 29, no. 1, pp. 113–123, 2006.

[41] O. Sorg, "Stress oxydant : un modele theorique ou une realite biologique ?," *Comptes Rendus Biologies*, vol. 327, no. 7, pp. 649–662, 2004.

[42] D. Dale, L. Boxer, and W. Liles, "The Pphagocytes: neutrophils and monocytes," *The Blood*, vol. 112, no. 4, pp. 935–945, 2008.

[43] S. Klebanoff, "Myeloperoxidase: friend and foe," *Journal of Leukocyte Biology*, vol. 77, no. 5, pp. 598–625, 2005.

[44] M. Adel, S. Yeganeh, M. Dadar, M. Sakai, and M. A. O. Dawood, "Effects of dietary *Spirulina platensis* on growth performance, humoral and mucosal immune responses and disease resistance in juvenile great sturgeon (*Huso huso* Linnaeus, 1754)," *Fish and Shellfish Immunology*, vol. 56, pp. 436–444, 2016.

[45] M. Abdel-Tawwab and M. H. Ahmad, "Live Spirulina (Arthrospira platensis) as a growth and immunity promoter for Nile tilapia, Oreochromis niloticus (L.), challenged with pathogenic Aeromonas hydrophila," *Aquaculture Research*, vol. 40, no. 9, pp. 1037–1046, 2009.

[46] H. Watanuki, K. Ota, A. Citra, M. A. R. Tassakka, T. Kato, and M. Sakai, "Immunostimulant effects of dietary *Spirulina platensis* on carp, *Cyprinus carpio*," *Aquaculture*, vol. 258, no. 1-4, pp. 157–163, 2006.

[47] A. D. Talpur and M. Ikhwanuddin, "Dietary effects of garlic (Allium sativum) on haematoimmunological parameters , survival, growth, and disease resistance against Vibrio harveyi infection in Asian sea bass, Lates calcarifer (Bloch)," *Aquaculture*, vol. 364-365, pp. 6–12, 2012.

[48] X. Geng, X. Dong, B. Tan et al., "Effects of dietary chitosan and *Bacillus subtilis* on the growth performance, non-specific immunity and disease resistance of cobia, *Rachycentron canadum*, Rachycentron Canadum," *Fish and Shellfish Immunology*, vol. 31, no. 3, pp. 400–406, 2011.

[49] A. Gopalakannan and V. Arul, "Immunomodulatory effects of dietary intake of chitin, chitosan and levamisole on the immune system of *Cyprinus carpio* and control of *Aeromonas hydrophila* infection in ponds," *Aquaculture*, vol. 255, no. 1-4, pp. 179–187, 2006.

[50] L. Luo, X. Cai, C. He, M. Xue, X. Wu, and H. Cao, "Immune response, stress resistance and bacterial challenge in juvenile rainbow trouts *Oncorhynchus mykiss* fed diets containing chitosan-oligosaccharides," *Current Zoology*, vol. 55, pp. 416–422, 2009.

[51] V. Aliko, M. Qirjo, E. Sula, V. Morina, and C. Faggio, "Antioxidant defense system, immune response and erythron profile modulation in gold fish, *Carassius auratus* , after acute manganese treatment," *Fish and Shellfish Immunology*, vol. 76, pp. 101–109, 2018.

[52] J. DeKoning and S. Kaattari, "Mitogenesis of rainbow trout peripheral blood lymphocytes requires homologous plasma for optimal responsiveness," *In Vitro Cellular & Development Biology*, vol. 27, no. 5, pp. 381–386, 1991.

[53] B. Wimer, "Putative effects of mitogenic lectin therapy corroborated by allo-activation data," *Cancer Biotherapy and Radiopharmaceuticals*, vol. 11, no. 1, pp. 57–75, 1996.

[54] E. Wattrang, A. Palm, and B. Wagner, "Cytokine production and proliferation upon in vitro oligodeoxyribonucleotide stimulation of equine peripheral blood mononuclear cells," *Veterinary Immunology and Immunopathology*, vol. 146, no. 2, pp. 113–124, 2012.

[55] B. Zhang, K. Zhao, W. He et al., "Study on optimal condition of MTT in PBMC transformation," *Progress Veterinary Medicine*, vol. 3, pp. 65–68, 2011.

[56] D. P. Anderson and M. G. Zeeman, "Immunotoxicology in Fish," in *In Fundamentals of Aquatic Toxicology: Effects, Environmental Fate & Risk Assessment. (G. Rand, Pp. 371–404)*, Taylor and Francis, Washington, DC, 1995.

[57] H. M. A. Abdelrazek, H. M. Tag, O. E. Kilany, P. G. Reddy, and A. M. Hassan, "Immuomodulatory effect of dietary turmeric supplementation on Nile tilapia (Oreochromis Niloticus)," *Aquaculture Nutrition*, vol. 23, no. 5, pp. 1048–1054, 2017.

[58] P. L. P. F. Carvalho, F. Y. Yamamoto, M. M. Barros, and D. M. Gatlin, "l-glutamine *in vitro* supplementation enhances Nile tilapia *Oreochromis niloticus* (Linnaeus, 1758) leukocyte function," *Fish and Shellfish Immunology*, vol. 80, pp. 592–599, 2018.

[59] S. Y. Shiau, J. Gabaudan, and Y. H. Lin, "Dietary nucleotide supplementation enhances immune responses and survival to *Streptococcus iniae* in hybrid tilapia fed diet containing low fish meal," *Aquaculture Reports*, vol. 2, pp. 77–81, 2015.

[60] W. C. Chuang, Y. C. Ho, J. W. Liao, and F. J. Lu, "Dunaliella salina exhibits an antileukemic immunity in a mouse model of WEHI-3 leukemia cells," *Journal of Agricultural and Food Chemistry*, vol. 62, no. 47, pp. 11479–11487, 2014.

[61] J. S. Park, J. H. Chyun, Y. K. Kim, L. L. Line, and B. P. Chew, "Astaxanthin decreased oxidative stress and inflammation and enhanced immune response in humans," *Nutrition and Metabolism*, vol. 7, no. 1, pp. 1–10, 2010.

[62] R. Harikrishnan, G. Devi, C. Balasundaram et al., "Effect of chrysophanic acid on immune response and immune genes transcriptomic profile in *Catla catla* against *Aeromonas hydrophila*," *Scientific Reports*, vol. 11, no. 1, pp. 1–15, 2021.

[63] J. Li, Z. Yuan, H. Liu, J. Feng, and Z. Chen, "Size-dependent tissue-specific biological effects of core–shell structured Fe3O4@SiO2– NH2 nanoparticles," *Journal of Nanobiotechnology*, vol. 17, no. 1, pp. 1–14, 2019.

[64] S. A. De Pascali, L. Del Coco, S. Felline, E. Mollo, A. Terlizzi, and F. P. Fanizzi, "1H NMR spectroscopy and MVA analysis of Diplodus argus eating the exotic pest Caulerpa cylindracea," *Marine Drugs*, vol. 13, no. 6, pp. 3550–3566, 2015.

[65] H. Gunther, "Chapter 10: More 1D and 2D NMR experiments," in *NMR Spectroscopy: Basic Principles, Concepts, and Applications in Chemistry*, vol. 3, pp. 341–376, Wiley-VCH Verlag GmbH & Co, Weinheim, Germany, 2013.

[66] B. Worley and R. Powers, "Multivariate analysis in metabolomics," *Current Metabolomics*, vol. 1, no. 1, pp. 92–107, 2013.

[67] G. Shen, J. Dong, K. Cheng, and J. Feng, "Metabolic effect of dietary taurine supplementation on Nile tilapia (Oreochromis nilotictus) evaluated by NMR-based metabolomics," *Journal of Agricultural and Food Chemistry*, vol. 66, no. 1, pp. 368–377, 2018.

[68] G. Shen, S. Wang, J. Dong, J. Feng, J. Xu, and F. Xia, "Metabolic effect of dietary taurine supplementation on grouper (Epinephelus coioides): a 1H-NMR-based metabolomics study," *Molecules*, vol. 24, no. 2253, pp. 1–16, 2019.

[69] L. Eriksson, E. Johansson, N. Kettaneh-Wold, J. Trygg, C. Wikstrom, and S. Wold, *Multi- and Megavariate Data Analysis Part 1: Basic Principles and Applications*, Umetrics Academy, Umeå, Sweden, 2006.

[70] S. Zhang, X. Zeng, M. Ren, X. Mao, and S. Qiao, "Novel metabolic and physiological functions of branched chain amino acids: a review," *Journal of Animal Science and Biotechnology*, vol. 8, no. 1, pp. 1–12, 2017.

[71] I. Ahmed and M. Khan, "Dietary branched-chain amino acid valine, isoleucine and leucine requirements of fingerling Indian major carp, Cirrhinus mrigala (Hamilton)," *British Journal of Nutrition*, vol. 96, pp. 450–460, 2006.

[72] M. Khan and S. Abidi, "Dietary isoleucine requirement of fingerling Indian major carp, Labeo rohita (Hamilton)," *Aquaculture Nutrition*, vol. 13, no. 6, pp. 424–430, 2007.

[73] M. S. A. Bustamam, H. A. Pantami, A. Azizan et al., "Complementary analytical platforms of NMR spectroscopy and LCMS analysis in the metabolite profiling of Isochrysis galbana," *Marine Drugs*, vol. 19, no. 3, p. 139, 2021.

[74] Y. Zhao, M. Y. Yan, Q. Jiang et al., "Isoleucine improved growth performance, and intestinal immunological and physical barrier function of hybrid catfish *Pelteobagrus vachelli* × *Leiocassis longirostris*," *Fish and Shellfish Immunology*, vol. 109, pp. 20–33, 2021.

[75] Y. Sharf and M. A. Khan, "Effect of dietary isoleucine level on growth, protein retention efficiency, haematological parameter, lysozyme activity and serum antioxidant status of fingerling Channa Punctatus (Bloch)," *Aquaculture Nutrition*, vol. 26, no. 3, pp. 908–920, 2020.

[76] M. Pasek, "Rethinking early earth phosphorus geochemistry," *Proceedings of the National Academy of Sciences of the USA*, vol. 105, no. 3, pp. 853–858, 2008.

[77] J. Wen, W. Jiang, L. Feng et al., "The influence of graded levels of available phosphorus on growth performance, muscle antioxidant and flesh quality of young grass carp (*Ctenopharyngodon idella*)," *Animal Nutrition*, vol. 1, no. 2, pp. 77–84, 2015.

[78] L. U. Gan, D. W. Jiang, P. Wu et al., "Flesh quality loss in response to dietary isoleucine deficiency and excess in fish: a link to impaired Nrf2-dependent antioxidant defense in muscle," *PLoS One*, vol. 9, no. 12, pp. 115–129, 2014.

[79] J. Brosnan and M. Brosnan, "Glutamate: a truly functional amino acid," *Amino Acids*, vol. 45, no. 3, pp. 413–418, 2013.

[80] R. Rezaei, D. Knabe, C. Tekwe et al., "Dietary supplementation with monosodium glutamate is safe and improves growth performance in postweaning pigs," *Amino Acids*, vol. 44, no. 3, pp. 911–923, 2013.

[81] D. Burrin and B. Stoll, "Metabolic fate and function of dietary glutamate in the gut," *The American Journal of Clinical Nutrition*, vol. 90, no. 3, pp. 850S–856S, 2009.

[82] A. Johnson, Y. Kaufmann, S. Luo, K. Babb, R. Hawk, and V. Klimberg, "Gut glutathione metabolism and changes with 7, 12-DMBA and glutamine," *Journal of Surgical Research*, vol. 155, pp. 242–246, 2003.

[83] J. Jiang, D. Shi, X. Zhou et al., "Effects of glutamate on growth, antioxidant capacity, and antioxidant-related signaling

molecule expression in primary cultures of fish enterocytes," *Fish Physiology and Biochemistry*, vol. 41, no. 5, pp. 1143–1153, 2015.

[84] Y. Zhao, Y. Hu, X. Q. Zhou et al., "Effects of dietary glutamate supplementation on growth performance, digestive enzyme activities and antioxidant capacity in intestine of grass carp (Ctenopharyngodon idella)," *Aquaculture Nutrition*, vol. 21, no. 6, pp. 935–941, 2015.

[85] S. W. Cho, H. Y. Yoon, J. Y. Ahn, E. Y. Lee, and J. Lee, "Cassette Mutagenesis of Lysine 130 of Human Glutamate Dehydrogenase. An Essential Residue in Catalysis," *European Journal of Biochemistry*, vol. 268, no. 11, pp. 3205–3213, 2021.

[86] J. Li, C. Wang, L. Wang et al., "Effects of glutamate in low-phosphorus diets on growth performance, antioxidant enzyme activity, immune-related gene expression and resistance to Aeromonas Hhdrophila of juvenile mirror carp (Cyprinus carpio)," *Aquaculture Nutrition*, vol. 26, no. 4, pp. 1329–1339, 2020.

[87] T. Barr, C. Helms, K. Grant, and I. Messaoudi, "Opposing effects of alcohol on the immune system," *Progress in Neuro-Psychopharmacology & Biological Psychiatry*, vol. 65, pp. 242–251, 2016.

[88] J. McClintick, J. Tischfield, L. Deng, M. Kapoor, X. Xuei, and H. Edenberg, "Ethanol activates immune response in lymphoblastoid cells," *Alcohol*, vol. 79, pp. 81–91, 2019.

[89] R. P. Donnelly and D. K. Finlay, "Glucose, glycolysis and lymphocyte responses," *Molecular Immunology*, vol. 68, no. 2, pp. 513–519, 2015.

[90] W. H. Wang, "The elastic properties, elastic models and elastic perspectives of metallic glasses," *Progress in Materials Science*, vol. 57, no. 3, pp. 487–656, 2012.

[91] F. Di Virgilio and E. Adinolfi, "Extracellular purines, purinergic receptors and tumor growth," *Oncogene*, vol. 36, no. 3, pp. 293–303, 2017.

[92] J. Yin, W. Ren, X. Huang, J. Deng, T. Li, and Y. Yin, "Potential mechanisms connecting purine metabolism and cancer therapy," *Frontiers in Immunology*, vol. 9, p. 1697, 2018.